Articles in PresS. J Neurophysiol (February 25, 2009). doi:10.1152/jn.90566.2008

Submitted to Journal of Neurophysiology-Revision 2

Differential Metabotropic Glutamate Receptor Expression and Modulation in Two Neocortical Inhibitory Networks

Qian-Quan Sun[1,2,*] Zhi Zhang[1], Yuanyuan Jiao[1,2], Chunzhao Zhang[1] and Gábor Szabó[3], Ferenc Erdelyi[3].

1. Department of Zoology and Physiology, University of Wyoming, Laramie, WY 82071. 2. Neuroscience Program, University of Wyoming, Laramie, WY 82071. 3. Laboratory of Molecular Biology and Genetics, Institute of Experimental Medicine, P.O. Box 67, H-1450 Budapest, Hungary.

* Author of correspondence should be addressed to Dr. Qian-Quan Sun, email neuron@uwyo.edu, telephone 307 766 5602, fax 307 766 5526.

Acknowledgement: We thank Dr. Yuchio Yanagawa at the Department of Genetic and Behavioral Neuroscience, Gunma University Graduate School of Medicine for the generous gift of GAD67-GFP mouse. This research was supported by National Institutes of Health grants 5R01NS057415 and P20 RR15640 (QQS). Confocal microscopy was performed in the University of Wyoming's Microscopy Core Facility. We thank Mr. Andrew Young and Jonathan Musser for providing editorial assistance.

Keywords: Interneuron; metabotropic glutamate receptors; cortex; GABAergic; GAD65 and GAD67.

Running title: Cell-type specific mGluR modulation in barrel cortex

Abstract

Taking advantage of transgenic mice with genetically labeled GABA-releasing interneurons, we examined the cell-specific patterns of mGluR expression in two broadly defined subtypes of inhibitory interneurons in layer IV of somatosensory cortex. Electrophysiological recording combined with application of specific agonists for specific mGluRs demonstrated different effects of mGluR activation in fast-spiking (FS) vs. regular spiking non-pyramidal (RSNP) interneurons. Whereas activation of group I, II and III mGluRs inhibited excitatory synaptic transmission in RSNP neurons predominantly via post-synaptic mechanisms, group I mGluR activation depolarized FS but not RSNP interneurons. Immunoreactivities of mGluR1, mGluR5, mGluR2/3 and mGluR8 exhibited different cellular expression patterns in the two groups of neurons which were not entirely consistent with physiological and pharmacological experiments. Taken together, our data indicate cell and circuit-specific roles for mGluRs in modulating inhibitory circuits in the somatosensory cortex. These results help to reinforce the concept that RSNP and FS cells represent morphologically, physiologically and functionally distinct groups of interneurons. The results reported here help to increase our understanding of the roles of mGluRs in endogenous glutamatergic induced plasticity of interneuronal networks.

Introduction

As the major excitatory neurotransmitter in the mammalian brain, glutamate can activate both fast excitatory synaptic potentials by ionotropic glutamate receptors (GluRs), and slow excitatory synaptic responses via metabotropic glutamate receptors (mGluRs; Conn & Pin, 1997; Salt, 2002; Wong et al., 2004). To date, eight mGluR subtypes (mGluR1-mGluR8) have been found in the mammalian brain and are classified into three groups with respect to their structural features, neuronal signaling and pharmacological properties (reviewed by Conn & Pin, 1997): 1) Group I mGluRs include mGluR1 (with alternative spliced variants, mGluR1a-g, Pin et al., 1992; Baude et al., 1993) and mGluR5 (with differently spliced forms, mGluR5a & b, Abe et al., 1992); 2) Group II mGluRs include mGluR2 and mGluR3; and 3) Group III mGluRs include mGluR4 and mGluR6-8 (Dalezios et al., 2002). At glutamatergic synapses, group I mGluRs are mainly postsynaptic receptors (Baude et al., 1993) involved in regulating glutamate release. In contrast, group II and III mGluR agonists are reported to presynaptically reduce glutamate or other neurotransmitter release (Calabreshi et a., 1993). All mGluR subtypes, excluding mGluR6, are expressed in the mammalian CNS (Nakajima et al., 1993). In the cerebral cortex, previous studies in rats have shown that mGluR1a is widely expressed in somatosensory cortex (SI) layers I-VI (Munoz et al., 1999). Furthermore, group I mGluR proteins (mGluR1a and mGluR5), are found in both symmetric and asymmetric synapses (Hubert et al., 2001; Lopez-Bendito et al., 2002; Petralia et al., 1997) in ventrobasal thalamus and

the cerebral cortex (Liu et al., 1998), suggesting an important role in regulating corticothalamic synaptic connections. In the ventral posterior thalamus and SI, group II mGluR proteins (mGluR2/3) are concentrated in neuronal somata, dendrites and synapses through the postnatal ages (Munoz et al., 1999; Liu et al., 1998). mGluRs are involved in many critical physiological processes including neuronal development, synaptic modulation, learning, memory (Con & Pin, 1997; Schoepp et al, 1999; Salt 2002), and neurological disorders such as epilepsy (Wong et al., 2004) and fragile-X syndrome (Bear et al., 2004). Expression of several mGluR isoforms has been reported in GABA releasing interneurons of the neocortex (Baude et al., 1993; Dalezios et al., 2002; Lujan et al., 1997). However, it is unclear how specific mGluRs regulate excitability and glutamate transmission in different interneurons. Because mGluR receptor mediated modulation is dependent on the postsynaptic target cells in hippocampal circuits (McBain, et al., 1994; Maccaferri et al., 1998; reviewed by Toth and McBain), it is very important to link the expression of mGluRs with their physiological functions in specific groups of interneurons. An expansion in the understanding of the target specific effects of mGluR in neocortical circuits is necessary in order to understand state-dependent information processing within the neocortex. Here, we took advantage of two functionally and structurally distinct types of interneurons (RSNP and FS) in the barrel cortex and examined whether there is any cell-type specific mGluR mediated modulation. The results help to increase our understanding of the roles of mGluRs in endogenous glutamatergic induced plasticity of interneuronal networks.

Materials and Methods

Animals and treatment groups Transgenic mice were generated to selectively and consistently express eGFP in distinct subpopulations of GABAergic neurons. In a GAD65-GFP strain (Lopez-Bendito et al., 2004), the expression of GFP was found predominantly in layer II-III, and to a smaller extent in layer IV. These cells also expressed calretinin (Lopez-Bendito et al., 2004; Zhang et al., 2006). In the layer IV barrel cortex, as well as in the piriform cortex (Zhang et al., 2006), all of the GAD65-GFP cells are physiologically identified as RSNP interneurons, whose axons innervate layer IV, V and II/III. In another strain, glutamate decarboxylase (GAD) 67-green fluorescent (GFP) (Δneo) mice (Tamamaki et al., 2003), GFP is selectively expressed under the control of the endogenous GAD67 gene promoter (Tamamaki et al., 2003; Jiao et al., 2006). In this strain, virtually all (~95%) GABAergic neurons expressed eGFP. In barrel cortex layer 4, 82% of the eGFP-positive neurons are fast-spiking, parvalbumin-positive, basket cells (Fig. 1), and the rest are predominantly RSNP cells. We used the **GAD65-eGFP mouse** and the **GAD67-eGFP mouse** to examine cell-type specific mGluR expression and modulation in the barrel cortex. At postnatal day 30 (P30), the GAD-GFP transgenic mice were given a lethal injection of Nembutal and perfused intracardially with 0.9% sodium chloride, followed by 4% paraformaldehyde. The brain was then removed, and the whole cortex was dissected. Thalamocortical (TC) sections were prepared based on methods described by Agmon and Connors (1991). Then the tissues were cryoprotected in 30% sucrose, and later cut into 40 μm sections to be processed for

fluorescent staining. TC sections were used to obtain an optimal barrel related expression pattern and barrel-specific intracellular electrophysiological recordings.

Immunohistochemistry and fluorescent labeling. Sections were incubated in 0.6% H_2O_2 for 30 minutes, PBS washed, switched to 50% alcohol for 10 minutes, PBS washed, then incubated in TBS with 0.5% Triton X-100, 2% BSA and 10% normal goat serum for 2 hours, and incubated in primary antibodies directed against the following: PV (parvalbumin ,1:1000, Millipore, Billerica, MA), mGluR1 (1:500, Millipore, Billerica, MA), mGluR2/3 (1:500, Millipore, Billerica, MA), mGluR5 (1:500, Millipore, Billerica, MA), mGluR8 (1:500, Millipore, Billerica, MA) and VGLUT2 (1:500, Millipore, Billerica, MA) overnight. The next day, after PBS rinsing, sections were incubated in Alexa Fluor 594, goat anti-rabbit IgG (heavy and light chains; 1:1000; Invitrogen, Carlsbad, CA) for mGluR1-8, Alexa Fluor 350, goat anti-mouse IgG (heavy and light chains; 1:1000; Invitrogen, Carlsbad, CA) for VGLUT2 and Alexa Fluor 594, goat anti-mouse IgG (heavy and light chains; 1:1000; Invitrogen, Carlsbad, CA) for PV, respectively, for 2 hours, then rinsed, mounted and coverslipped. The specificity of mGluR immunolabeling was verified in control experiments by preabsorption of the mGluR receptor antibody with antibody specific control peptides which resulted in the complete absence of immunolabeling. The immunofluorescent specimens were examined with an epifluorescence microscope (Zeiss, Thornwood, NY) equipped with an AxioCam digital CCD camera. Double and triple immunofluorescent images were taken under confocal fluorescence microscopy. Confocal microscopy was performed in the UW Microscopy CORE

Facility. An upright Nikon E800 microscope was used as Confocal Laser Scanning Microscope (Bio-Rad Radiance 2100). Laser lines include: blue diode laser (405 nm); argon ion laser (457, 477, 488, and 514 nm); HeNe Laser (543 nm); Red diode laser (637 nm). Thin optical sections (< 1μm) and small pinholes (0.2-0.4 μm) were used during confocal image sampling process to optimize local fluorescent signaling of mGluR expression levels in single cells. AxioVision LE imaging suite (Carl Zeiss) software, and its Automeasure® program, were used to study fluorescent intensities near neurons and measure grayscale intensities for mGluRs. Relative values of mGluR-IR (grayscale intensities) were compared only between cells (PV+ vs. PV-) which were located in the same optical section. Therefore fluorescent intensity was shown as relative values on a 100% scale.

Brain slice preparations and electrophysiological recordings. GAD67-GFP and GAD65-GFP mice (age: postnatal 25-30 days) were deeply anesthetized with pentobarbital sodium (55 mg/kg) and decapitated. The brains were quickly removed and placed into cold (~4°C) oxygenated slicing medium containing (in mM): 2.5 KCl, 1.25 NaH_2PO_4, 10.0 $MgCl_2$, 0.5 $CaCl_2$, 26.0 $NaHCO_3$, 11.0 glucose, and 234.0 sucrose. TC slices were prepared according to methods described by Agmon and Connors (Agmon and Connors, 1991). Tissue slices (300-400 μm) were cut using a vibratome (TPI, St. Louis, MO), transferred to a holding chamber, and incubated (35°C) for at least 1 hour. Individual slices were then transferred to a recording chamber, fixed to a modified microscope stage, and allowed to equilibrate for at least 30 min before recording. Slices were minimally submerged and continuously

superfused with oxygenated physiological saline at the rate of 4.0 ml/min. The physiological perfusion solution contained (in mM): 126.0 NaCl, 2.5 KCl, 1.25 NaH_2PO_4, 1.0 $MgCl_2$, 2.0 $CaCl_2$, 26.0 $NaHCO_3$, and 10.0 glucose. Solutions were gassed with 95% O_2/5% CO_2 to a final pH of 7.4 at a temperature of 35 ± 1°C. The method for identification of the barrel subfield in living TC slices was described in earlier studies (Sun et al., 2006). A low-power objective (2.5×) was used to identify barrels and thalamic nuclei, and a high-power water immersion objective (40×) with Nomarski optics and infrared video was used to visualize individual neurons. Recording pipettes were fabricated from capillary glass obtained from World Precision Instruments (M1B150F-4), using a Sutter Instrument P80 puller, and had tip resistances of 2-5 MΩ when filled with the intracellular solutions below. A Multi-clamp 700B amplifier (Axon Instruments, Foster City, CA) was used for voltage-clamp and current clamp recordings. Patch pipette saline was modified according to Brecht and Sakmann (Brecht and Sakmann, 2002) and composed of (in mM): 100 K-gluconate, 10.0 phosphocreatine-Tris, 3.0 $MgCl_2$, 0.07 $CaCl_2$, 2 EGTA, 10.0 HEPES, 4.0 Na_2-ATP, and 1.0 Na-GTP, pH adjusted to 7.4 and osmolarity adjusted to 280 $mosMl^{-1}$. Neurobiotin (0.5%; Vector Labs) was regularly added to the patch pipette solution. Current and voltage clamp protocols were generated using PCLAMP9.2 software (Axon Instruments). Cells with a resting membrane potential value less negative than -50 mV were arbitrarily rejected for further investigation to eliminate cells with poor quality of seal. In voltage clamp recordings, series resistance values smaller than 10MΩ were deemed acceptable. Series resistance was usually compensated using multi-clamp automated compensation function. In

voltage-clamp recordings, because a fixed holding voltage (usually -70 mV) was used, the holding current varied based on the actual resting membrane potential of the cell, series resistance and the input resistance. Spike frequency: the reciprocal of the first interspike interval (ISI). Frequency (initial, Hz): the reciprocal of the first ISI, measured at the smallest threshold current step which induced spikes. Frequency (maximal or 250 pA, Hz): the reciprocal of the first ISI, measured at the 250 pA current step. All cells were filled with biocytin. Cells were routinely processed for co-exression of PV or another interneuron marker. A sharpened bipolar tungsten electrode, placed carefully at ~100 μm away laterally from recorded cells in the cortical layer IV, was used to activate intracortical fibers. Monosynaptic excitatory postsynaptic currents (EPSCs) were evoked in interneurons with the stimuli and were recorded at holding potential of -80mV. eEPSCs were evoked in the presence of a cocktail ACSF solution containing $GABA_A$ antagonist picrotoxin (50 μM) and low concentration of AMPA/kainite receptor antagonist 2,3-dihydro-6-nitro-7-sulfamoyl-benzo(F) quinoxaline (NBQX; 0.1 μM) to reduce excitation and prevent hyper-excitability (Kumar and Huguenard, 2001). Miniature EPSCs were recorded in the presence of TTX (100 nM). Spontaneous EPSCs (sEPSCs) were recorded in the presence of picrotoxin and the absence of TTX. Detection and analysis of mEPSCs and sEPSCs were performed using clampfit® (version 9.2), event detection function. First a mEPSCs (or sEPSC) template was created from 10 representative mEPSCs events. The program then searched the entire recording periods (~10 minutes) against the defined template with a match threshold of 5-6. Events with amplitudes larger than 2.5x noise level were accepted and analyzed. Chemicals: AMPA

antagonist GYKI 52466 hydrocloride, [1-(4-aminophenyl)-4-methyl-7, 8-methylenedioxy-5H-2, 3-benzodiazepine] (Sigma-Aldrich, St. Louis, MO 63178); NBQX (Tocris. Ellisville, Missouri 63021), DL-AP5 (Tocris), ifenprodil (NR2B antagonist, Tocris), Picrotoxin (Tocris), SR95531 (Tocris), and TTX (Sigma). Selective agonist of mGluRs (Tocris; reviewed by Schoepp et al, 1999, Conn & Pin, 1997): (±)-trans-ACPD [(±)-1-Aminocyclopentane-trans-1,3-dicarboxylic acid, group I/ II mGluRs]; (RS)-3,5-DHPG [(RS)-3,5-Dihydroxyphenylglycine; group I mGluR agonist]; L-AP4 [L-(+)-2-Amino-4-phosphonobutyric acid; selective group III mGluR agonist]; APDC [(2R,4R)-4-Aminopyrrolidine-2,4-dicarboxylate; a highly selective and relatively potent group II mGluR agonist]. CHPG: [(RS)-2-Chloro-5-hydroxyphenylglycine; a selective mGlu5 receptor agonist]. Selective antagonist for mGluRs: AIDA [(RS)-1-Aminoindan-1,5-dicarboxylic acid; selective antagonist of group I mGluR]; LY341495: [(2S)-2-Amino-2-[(1S,2S)-2-carboxycycloprop-1-yl]-3-(xanth-9-yl) propanoic acid; selective antagonist of group II mGluR]; MSPG: [(RS)-α-Methyl-4-sulfonophenylglycine. **Statistics:** Paired (or unpaired) T-test and One-Way Anova analyses were used to examine statistical significance and $p<0.05$ was considered to be significantly different.

Results

Two subtypes of interneurons are distinguished by firing properties. We used two strains of GAD-GFP mice to improve the success rate for differentiating physiologically distinct interneurons. In the GAD65-GFP mice, the PV containing subpopulation of interneurons do not express GFP but the regular spiking non-

pyramidal (RSNP) cells do (Fig 1). On the other hand, in the GAD67-GFP mice most of the GFP expressing interneurons are PV-positive (Fig 1). This correlation is further characterized with electrophysiological recordings (Fig1&2). Based on this difference in the cell type-specificity in GFP expression, 100% of the GFP positive neurons in the GAD65-GFP mice were RSNP interneurons (Fig 1, n=20). In contrast, 82±5% GFP-positive cells (n=23) from the GAD67-GFP mice were fast-spiking (FS) interneurons (Fig 1). In 8/8 GAD67-GFP and PV+ positive cells (100%), all were found to exhibit FS firing properties (Fig.1D2 &E2). Thus the two populations of GFP positive interneurons (GAD65 &GAD67) were used to improve success rates for recording from physiologically distinct interneurons (RSNP vs. FS). RSNP cells generated adapting trains of spikes (e.g. Fig. 1), a lack of fast AHPs (e.g. Fig. 1), a modest maximum (300 pA) firing rate of 48±6 Hz and each spike had a relatively long AP-width (1.4 ±0.3 ms, n=16). In contrast, FS cells usually had maximum (300 pA) firing rates of 195±14 Hz, large fast AHPs (18±2 mV), narrow APs (AP half-width value 0.4±0.04 ms) and on average displayed no spike-frequency adaptation (e.g. Fig. 1). The near threshold firing frequency for RSNP neurons was 14 ± 4 Hz (n=20), which was much slower than the near threshold firing frequency of FS cells (61±3 Hz, n=20, $p<0.01$). Cells with both maximum (i.e. induced by 300pA step current) firing frequencies of larger than 150 Hz and a spike half-width of less than 0.7 ms were classified as FS cells (Bacci et al., 2003; Beierlein et al., 2003). All other GAD67-GFP cells were defined as RSNP cells. Based on this criteria, FS cells and RSNP cells showed clearly distinct firing properties as well as synaptic properties. Bursting cells (or low-threshold spiking, LTS, ref) were also described in rat

neocortex (Bacci et al., 2003; Beierlein et al., 2003). However, we have never encountered a single LTS cells in barrel cortex layer IV barrels of GAD65- or GAD67-GFP mice. In addition to differences in their firing properties, these cells exhibited different morphological properties. While axons of FS cells are much more abundant than RSNP cells (Fig 2), dendrites of RSNP cells cover a much larger area than FS cells (Fig 2, n=6 in RSNP and n=4 FS cells). These differences provide an opportunity for studying the cell-type specific effects of mGluRs.

Distribution of mGluR receptors in GAD65-GFP neurons. Abundant mGluR expression has previously been reported in the barrel cortex layer IV (Munoz et al., 1999; Liu et al., 1998). To examine whether there was interneuron specific expression, we examined the co-expression of mGluRs in GABAergic interneurons. All GAD65-GFP neurons were RSNP neurons (Fig 1&2, cf. Zhang et al., 2006) and did not express PV (Fig 1A &D2). In contrast, the expression of PV was always consistent with the FS firing types in layer IV (n=8 100%, Fig 1D1 vs. D2). We next examined the expression of mGluRs in these cells. As shown in Fig 3, the expression of mGluR2/3 (Group II) and mGluR5 (Group I) were more abundant in the GAD65-GFP interneurons than PV+ neurons, suggesting that these receptors were more abundant in RSNP cells than FS cells. The mGluR1 receptors were also found in both GAD65-GFP (not shown) and PV+ cells (Fig 4D1 &E1), however, there were stronger mGluR-IR in PV+ cells (Fig 3C1). Furthermore, large, puncta-like expressions of mGluR2/3 & 5 were identified in large dendrites and soma region of these interneurons (e.g. Fig 3A2 &B2), raising the possibility that these mGluRs may

be functionally relevant to the synaptic release of glutamate. In addition, we found that the mGluR8 expression was modest in GAD65-GFP cells (data not shown). The expression pattern of mGluR8 was similar to mGluR5 (cf. Fig 3B2).

Distribution of mGluR receptors in GAD67-GFP and parvalbumin (PV)-positive interneurons. In GAD67-GFP mouse, >95% of GABAergic cells express GFP under the promoter of GAD67 in motor cortex (Tamamaki et al., 2003) and somatosensory cortex (Jiao et al., 2006). 81±5% of GFP positive interneurons are also PV positive and fast-spiking in layer IV barrel cortex (Jiao et al., 2006). We therefore examined the expression of mGluR in GAD67-GFP neurons. As shown in Fig 4, abundant mGluR1-IR expression at the somatic area of GAD67-GFP positive cells (Fig 4A2 & D1), as well as the large dendrites of GAD67-GFP negative cells (Fig 4D1), indicates a potential role in the regulation of neuronal excitability. In addition, modest levels of mGluR8, but not mGluR5, were also detected in the somatic area of GAD67-GFP neurons (Fig 4B2 & C2). mGluR2/3 was not expressed in the somatic area of GAD67-GFP cells. To further validate cell-specific expression of mGluRs in FS interneurons, slices from GAD67-GFP mouse were triple labeled with antibodies of various mGluR receptors (mGluR1, 2/3, 5&8). A third monoclonal antibody against the calcium binding protein, PV was used to label fast-spiking and basket interneurons in layer IV barrel cortex (Jiao et al., 2006). We have found significant expression of mGluR1 (similar to Fig 4A2, D1&E1) and modest expression of mGluR8 in the PV positive neurons (Fig 4D3 &E). The pattern of expression of mGluR1&5 was similar (Fig 4D1 vs. D2): large puncta-like expressions

were identified in large dendrites (longer than 2μm) of these interneurons as well as GFP-negative dendritic-like structures (Fig 4D1&2). In contrast, the mGluR8 & 2/3 were found both in large dendritic-like puncta (longer than 2μm), as well as in more discrete small puncta like structures which were not colocalized with GFP-positive small puncta (e.g. Fig 4D3 &Fig 3A2). The relative level of expression between PV+ and PV- neurons were compared among mGluR1, 5, 2/3 & 8. Similar differences were found in GAD67-GFP neurons and GAD65-GFP neurons (Fig 4E vs. Fig 3 C).

mGluR receptors differentially regulate excitatory synaptic transmission and intrinsic membrane conductance in RSNP vs. FS interneurons. We examined the effects of receptor specific exogenous mGluR agonists on the eEPSCs and intrinsic membrane conductance in RSNP and FS cells. First, we studied the effects of group I mGluR5 agonist, CHPG (Doherty et al., 1997), on spontaneous EPSCs (sEPSCs) in RSNP and FS cells (supplemental Fig 3). Our results showed that CHPG (1mM) induced small but significant changes in the amplitudes of the sEPSCs in RSNP (25±5%, n=6, $p<0.05$) and FS cell groups (18±5%, n=6, $p<0.05$; see supplemental Fig 3). There was a significant increase in the frequencies of sEPSCs recorded in both RSNP (87±7%, n=6, $p<0.01$) and FS cells (45±8%, n=6, $p<0.01$; see supplemental Fig 3). To investigate whether the effects of CHPG on sEPSCs frequency and amplitudes were mediated via different mechanism, we next examined the effects of CHPG on mEPSCs. As shown in Fig 6, CHPG had a significant inhibitory effect on the amplitudes but not the frequency of mEPSCs in both FS and RSNP cells (Fig 6), suggesting that the effects of CHPG on amplitudes

of mEPSCs are mediated predominantly via postsynaptic mechanisms. In contrast, the increase in sEPSC frequency disappeared in TTX, suggesting that it was mediated via an excitatory effect on spontaneous firing rate in glutamatergic neurons. We next examined the effects of CHPG (1 mM) on electrically evoked EPSCs in RSNP vs. FS cells (Fig. 6). In cells with RSNP firing properties, local perfusion of CHPG (1mM) induced rapid and reversible inhibition of eEPSCs (Fig. 6A2, 41±7% inhibition; n=6, $p<0.01$ vs. controls). In FS cells, CHPG, at the same concentration, had a similar but smaller effect on the eEPSCs in 4/6 FS cells (e.g. Fig. 6B2, 19±8%, $p<0.05$, n=31). In both RSNP and FS cells, the CHPG had no significant effects on the paired-pulse ratio (PPR) of the eEPSCs (Fig 6A3, B3 &C2), suggesting that the effects were predominantly postsynaptic and the increase of sEPSC frequencies occurred via an indirect effect on excitability of glutamatergic neurons. CHPG induced robust inward current in 6/6 FS cells (e.g. Fig. 6B1&2, C3, $p<0.001$). In the majority (5/6) of RSNP cells, there were no significant effect of CHPG on the intrinsic conductance which was measured simultaneously with synaptic potentials under voltage clamp (Fig 6A &C3; n=6, $p>0.1$). On average, the CHPG induced currents were 103±9 pA in FS cells but only 9±3 pA in RSNP cells (Fig 6C3, $p<0.001$ RSNP vs. FS). Thus CHPG differentially modulates FS and RSNP cells. To examine the specificity of CHPG mediated effects, we applied group I receptor antagonist AIDA. In slices pre-incubated with AIDA, CHPG did not change either the amplitudes of EPSCs or the holding currents (n=3 FS cells, data not shown).

We then studied the effects of group III mGluR receptor agonist L-AP4 (Con & Pin, 1997; Schoepp et al, 1999; Salt, 2002), on eEPSCs in RSNP and FS cells (Fig 7). Our results showed that L-AP4 (100 μM) induced significant inhibitory effects on the amplitudes of the eEPSCs in RSNP (48±6%, n=9, $p<0.001$) and FS cell groups (40±8%, n=8, $p<0.01$; Fig 7A1, B1 & D1). Despite the large effect on amplitude, there was no significant effect on PPR (Fig 7D2). This result suggests that similar to CHPG, L-AP4's effect occurs postsynaptically in interneurons. Unlike CHPG, L-AP4 had no effect on holding currents in both FS cells and RSNP cells (Fig 7A1&B1, Fig 8A2&B2), suggesting that group III and group I mGluR receptors activate different downstream second messengers. To test these possibilities, we examined whether the effects of CHPG on eEPSCs and holding currents were occluded by L-AP4 application. As shown in Fig 8A1&2, application of CHPG had additional effects on both eEPSCs in RSNP (62±5% vs. 44±6%, n=5, $p<0.05$) and FS cells (56±5% vs. 36±5%, n=5, $p<0.05$) and holding currents in FS cells (45±6 vs. 4±1pA, n=5, $p<0.01$) but not RSNP cells (3±1 vs. 10±1 pA, n=5, $p>0.1$; Fig 8B1&B2). These results suggest that at postsynaptic sites of glutamate synapses, group III and group I mGluR receptors may not have entirely convergent inhibitory effects on AMPA mediated EPSCs.

To further examine pharmacological profiles of mGluR mediated modulation on EPSCs, we applied group I mGluR agonist (RS)-3,5-DHPG (DHPG, Schoepp et al., 1999) and group II mGluR agonist (2R,4R)-APDC (APDC; Schoepp et al., 1999). Among these agonists, the effects of CHPG and L-AP4 on eEPSCs were mimicked

by DHPG (n=8 in RSNP cells and N=6 in FS cells, Fig 8C1&C2) and to a much smaller magnitude by APDC (n=7 in RSNP cells, $p<0.05$; n=10 in FS cells, $p<0.05$; Fig 8C). In addition, both receptor agonists (i.e. DHPG & APDC) appeared to inhibit the eEPSCs without affecting the PPR (not shown).

In voltage-clamp, CHPG induced robust effects on holding currents of FS cells but not RSNP cells. We further examined this effect under current clamp. As shown in Fig 9, application of group I/II mGluR receptor agonist (±)-trans-ACPD induced robust depolarization in FS cells. These depolarizations were usually very strong, because despite inhibitory effects on eEPSCs, (±)-trans-ACPD often enhanced both spontaneous firings and TC-induced spikes (Fig 9A2). (±)-trans-ACPD induced robust conductance changes in FS but not in RSNP cells (Fig 9B1). This effect was mimicked by group I mGluR agonists DHPG, CHPG, but not by group II agonist APDC or group III agonist L-AP4. The effect of (±)-trans-ACPD on conductance was blocked by selective group I receptor antagonist, AIDA (Fig 9B2), but not by group II antagonist LY341495 or the nonselective mGluR antagonist, MSPG. Together these results suggest that group I mGluRs, but not other mGluRs mediate the depolarization effect in FS cells.

Discussion

Our first significant finding was that mGluRs differentially modulate two different interneuronal types within somatosensory cortex. Because RSNP cells and FS cells form gap junctionally connected networks (Beierlein et al., 2003), their differential

modulation has important functional implications. Whereas in subcortical circuits, the effect of mGluRs on inhibitory circuits has well defined target-specific actions, i.e. distinct mGluRs have distinct functions based on their postsynaptic target interneurons (Desai et al., 1994; Toth and McBain, 2000; McBain and Fisahn, 2001; Pelkey et al., 2005), it is unclear whether a similar situation occurs in neocortical inhibitory circuits. Taking advantage of two strains of mice in which specific groups of GABAergic cells express GFP, we examined whether there is a cell-specific synaptic modulation and expression of mGluR in layer IV barrel cortex.

Using whole-cell patch clamp recording methods, local application of mGluR5 agonist, CHPG (Doherty, et al., 1997), induced very robust inhibitory effect on eEPSCs in RSNP cells, but had little effect on the intrinsic conductance in RSNP cells (Fig 6). In FS cells, CHPG had smaller effect on eEPSCs, but instead it evoked large changes in holding currents and conductance (Fig 6). In both RSNP and FS cells, the CHPG had no significant effects on the paired-pulse ratio (PPR) of the eEPSCs (Fig 6A3, B3 &C2), and frequency of mEPSCs, suggesting that the effects were predominantly postsynaptic. The effects of CHPG on miniature and spontaneous EPSCs are consistent with a postsynaptic action. mGluR1 agonist DHPG, had similar effects to CHPG on conductance in FS and RSNP cells and EPSCs in RSNP cells, but did not produce significant inhibition of EPSCs in FS cells (Fig 8). Local application of group I/II mGluR receptor agonist (±)-trans-ACPD induced a very robust (>55%) inhibitory effect on eEPSCs in RSNP cells but not in FS cells. (±)-trans-ACPD had little effect on the intrinsic conductance in RSNP cells. These results suggest that group I mGluRs differentially modulate conductance and

EPSCs in RSNP and FS cells. Other experiments (sEPSCs/mEPSCs and PPR) further suggest that a postsynaptic mechanism was involved. In hippocampus the effects of group I mGluRs are presynaptic, although the receptors may be located postsynaptically or even on other nearby neurons (Gereau and Conn, 1995). In contrast, the reduction in synaptic response size shown here appears to be occurring postsynaptically. Group II mGluR agonist APDC had only the smallest effects on eEPSCs in RSNP and FS cells. It did not produce any significant effects on intrinsic excitabilities. Group III mGluR agonist L-AP4 had an inhibitory effect on EPSCs in RSNP and FS cells. This effect appears to be similar to that mediated by CHPG, i.e. a predominant postsynaptic mechanism (Fig 7). Together, these data suggest that different mGluRs differentially modulate RSNP and FS cells. Group I & III mGluRs inhibit excitatory synaptic transmission predominantly via a postsynaptic mechanism. Group I receptors (mGluR1 & 5) also modulate intrinsic conductances in FS cells. The effect of mGluR1 & 5 in FS cells is similar to the effects in hippocampal circuits, where group I mGluRs induced a depolarization of O/A interneurons (McBain et al., 1994; Gee and Lacaille, 2004), and exerted excitatory effects on CA1 pyramidal cells by increasing cell firing (Mannaioni et al., 1999) and decreasing GABA-mediated inhibition (Gereau and Conn, 1995; Fitzsimonds and Dichter, 1996). The effects of group I & III mGluRs on excitatory synaptic transmission were also similar to hippocampus, where group I & III agonists also inhibit glutamatergic transmission at the Schaffer collateral--CA1 synapses via a similar mechanism (Gereau and Conn, 1995). However, analysis of the effects of agonists of these two receptors on miniature EPSCs and paired-pulse facilitation

suggest that both receptors are localized presynaptically (Gereau and Conn, 1995), which is different from our results. In neonatal rat hippocampus, group I mGluRs also inhibit EPSCs via a presynaptic mechanism (Baskys and Malenka, 1991). In another study, we found that endogenous activation of these receptors mediated LTD as well (Young and Sun, 2007). We suspect the downstream target of group I mGluRs, PLC/IP3-mediated dendritic Ca^{2+} mobilization, to be responsible because this postsynaptic mechanism was responsible for mGluR1 induced LTD in cerebellum (Kim et al., 2007). The postsynaptic inhibitory effects were also mimicked by group III agonist L-AP4. Although both group I and III mGluR agonists induced similar effects on glutamatergic transmission via a postsynaptic mechanism, the intracellular mechanisms could be very different. Group III mGluRs are known to inhibit G-protein mediated increase in intracellular cAMP and adenylyl cyclase (Con and Pin, 1997). This mechanism was shown to mediate a presynaptic inhibition of glutamate release by group III mGluRs (Cai et al., 2001). We suspect a similar action in the postsynaptic sites of neocortical inhibitory circuits that has not yet been reported.

In a few earlier studies, the two physiologically distinct groups of interneurons (RSNP vs. FS) are shown to exhibit dichotomy in several aspects including: formation of two distinct and gap junctionally connected networks in layer IV (Beierlein et al., 2003), differential short-term-plasticity (Beierlein et al., 2003), distinct $GABA_A$ receptor mediated IPSCs (Bacci et al., 2003), and endocannabinoid mediated responses (Bacci et al., 2004). The observed differences in mGluR

sensitivity and pharmacology thus add another example of this dichotomy. Together with these previous results (Bacci et al., 2003; and Beierlein et al., 2003), our results help to reinforce the concept that RSNP and FS cells represent morphologically, physiologically and functionally distinct groups of interneurons.

Our second significant finding was to provide immunohistochemical evidence regarding the differential mGluR expression in the two distinct interneuronal networks. The close correlation of firing property (RSNP and FS) with distinct genetically labeled GFP neurons and expression of calcium binding protein, PV, helped us determine the cell-specific expression of mGluRs. While 100% GAD65-GFP cells are RSNP cells and PV negative cells (Fig 1), 100% PV positive cells exhibit FS but not RSNP firing properties (Fig 1). This is extremely convenient for us to study cell-specific expression of mGluRs. Indeed, we found that the level and pattern of expression of different mGluRs in PV vs. non-PV cells was consistent with our pharmacological experiments. For example, in RSNP cells, mGluR2/3 and 5 & 8 were all expressed in postsynaptic (somatodendritic) sites of PV negative and GAD65-GFP positive cells (Fig 7), consistent with a electrophysiological data which indicate postsynaptic effects of these receptors on glutamate transmission. In contrast, in PV positive cells, these receptors (i.e. mGluR2/3 and 5) were expressed at a significantly lower level (Fig 3C&4D). In contrast, mGluR1 expression was significantly higher and was found at the soma and dendrites (as apposed to puncta e.g. MGluR2/3), which was also consistent with the role of mGluR1 agonist induced membrane depolarization in FS cells (i.e. PV positive cells). mGluR2/3-IR was

stronger in puncta form in RSNP cells (Fig 3C2), which is consistent with a bigger effect of APDC on EPSCs in RSNP cells than FS cells (Fig 8C). However, the expression level of mGluR5 was inconsistent with the immuno-staining pattern. Although CHPG induced robust depolarizations in FS but not RSNP cells, the mGluR5-IR appears to be stronger in PV negative cells and GAD65-GFP positive cells (Fig 3 &4).

The third significance of these results was that these findings will help to provide several hypothesis regarding significant functional roles of mGluRs in somatosensory circuits. 1) Glutamate transmissions onto RSNP are more likely to be down-regulated if mGluRs are activated. 2) Because RSNP cells project to dendrites of layer II/III cells and layer V cells, while FS cell projections are largely confined within layer IV barrels (cf. Fig 2, Sun et al., 2006), the differential effects of glutamate on their (RSNP vs. FS) excitabilities could serve as a switch to facilitate intra-barrel inhibition (mediated by FS cells) and inhibit inter-barrel inhibition (mediated by RSNP cells). 3) The differential mGluR modulation may serve as a mechanism of selective circuit activation during glutamate spillover, because mGluRs are usually extrasynaptic and can only be activated during intense level of activation of excitatory inputs (Sekizawa & Bonham, 2006). 4) Alternatively, if the ambient glutamate levels are altered during certain brain states (cf. Sandstrom & Rebec, 2007), different inhibitory networks (RSNP and FS) could also be differentially activated with higher levels of glutamate favoring activation of FS networks. Because FS cells and RSNP cells form functional networks via gap junction connections (Beierlein et al., 2003), their selective activation will have large effects on the entire

somatosensory cortex. FS cells are a major player of sensory-mediated feed-forward inhibition (Sun et al., 2006). mGluR activation will thus facilitate feed-forward inhibitory effects and produce larger inhibition of receptive field properties, presumably resulting in enhanced spatial resolution.

Reference List

1. Agmon A, Connors BW (1991) Thalamocortical responses of mouse somatosensory (barrel) cortex in vitro. Neuroscience 41: 365-379.

2. Abe T, Sugihara H, Nawa H, Shigemoto R, Mizuno N, Nakanishi S (1992) Molecular characterization of a novel metabotropic glutamate receptor mGluR5 coupled to inositol phosphate/Ca2+ signal transduction. J Biol Chem 267: 13361-13368.

3. Bacci A, Huguenard JR, Prince DA (2004) Long-lasting self-inhibition of neocortical interneurons mediated by endocannabinoids. Nature 431: 312-316.

4. Bacci A, Rudolph U, Huguenard JR, Prince DA (2003) Major differences in inhibitory synaptic transmission onto two neocortical interneuron subclasses. J Neurosci 23: 9664-9674.

5. Baskys A, Malenka RC (1991) Agonists at metabotropic glutamate receptors presynaptically inhibit EPSCs in neonatal rat hippocampus. J Physiol 444: 687-701.

6. Baude A, Nusser Z, Roberts JD, Mulvihill E, McIlhinney RA, Somogyi P (1993) The metabotropic glutamate receptor (mGluR1 alpha) is concentrated at perisynaptic membrane of neuronal subpopulations as detected by immunogold reaction. Neuron 11: 771-787.

7. Bear MF, Huber KM, Warren ST (2004) The mGluR theory of fragile X mental retardation. Trends Neurosci 27: 370-377.

8. Beierlein M, Gibson JR, Connors BW (2003) Two dynamically distinct inhibitory networks in layer 4 of the neocortex. J Neurophysiol 90: 2987-3000.

9. Brecht M, Sakmann B (2002) Dynamic representation of whisker deflection by synaptic potentials in spiny stellate and pyramidal cells in the barrels and septa of layer 4 rat somatosensory cortex. J Physiol 543: 49-70.

10. Cai Z, Saugstad JA, Sorensen SD, Ciombor KJ, Zhang C, Schaffhauser H, Hubalek F, Pohl J, Duvoisin RM, Conn PJ (2001) Cyclic AMP-dependent protein kinase phosphorylates group III metabotropic glutamate receptors and inhibits their function as presynaptic receptors. J Neurochem 78: 756-766.

11. Calabresi P, Pisani A, Mercuri NB, Bernardi G. (1993) Heterogeneity of metabotropic glutamate receptors in the striatum: electrophysiological evidence. Eur J Neurosci. 5:1370-7.

12. Conn PJ, Pin JP. (1997) Pharmacology and functions of metabotropic glutamate receptors. Annu Rev Pharmacol Toxicol. 37: 205-37.

13. Dalezios Y, Lujan R, Shigemoto R, Roberts JD, Somogyi P (2002) Enrichment of mGluR7a in the presynaptic active zones of GABAergic and non-GABAergic terminals on interneurons in the rat somatosensory cortex. Cereb Cortex 12: 961-974.

14. Desai MA, McBain CJ, Kauer JA, Conn PJ (1994) Metabotropic glutamate receptor-induced disinhibition is mediated by reduced transmission at excitatory synapses onto interneurons and inhibitory synapses onto pyramidal cells. Neurosci Lett 181: 78-82.

15. Doherty AJ, Palmer MJ, Henley JM, Collingridge GL, Jane DE (1997) (RS)-2-chloro-5-hydroxyphenylglycine (CHPG) activates mGlu5, but no mGlu1, receptors expressed in CHO cells and potentiates NMDA responses in the hippocampus. Neuropharmacology 36: 265-267.

16. Fitzsimonds RM, Dichter MA (1996) Heterologous modulation of inhibitory synaptic transmission by metabotropic glutamate receptors in cultured hippocampal neurons. Journal of Neurophysiology 75: 885-893.

17. Gee CE, Lacaille JC (2004) Group I metabotropic glutamate receptor actions in oriens/alveus interneurons of rat hippocampal CA1 region. Brain Research 1000: 92-101.

18. Gereau RW, Conn PJ (1995) Multiple Presynaptic Metabotropic Glutamate Receptors Modulate Excitatory and Inhibitory Synaptic Transmission in Hippocampal Area Ca1. Journal of Neuroscience 15: 6879-6889.

19. Hubert GW, Paquet M, Smith Y (2001) Differential subcellular localization of mGluR1a and mGluR5 in the rat and monkey Substantia nigra. J Neurosci 21: 1838-1847.

20. Jiao YY, Zhang CZ, Yanagawa Y, Sun QQ (2006) Major effects of sensory experiences on the neocortical inhibitory circuits. Journal of Neuroscience 26: 8691-8701.

21. Jin Y, Kim SJ, Kim J, Worley PF, Linden DJ (2007) Long-term depression of mGluR1 signaling. Neuron 55: 277-287.

22. Kumar SS, Huguenard JR. (2001) Properties of excitatory synaptic connections mediated by the corpus callosum in the developing rat neocortex. J Neurophysiol. 86:2973-85.

23. Liu XB, Munoz A, Jones EG (1998) Changes in subcellular localization of metabotropic glutamate receptor subtypes during postnatal development of mouse thalamus. J Comp Neurol 395: 450-465.

24. Lopez-Bendito G, Sturgess K, Erdelyi F, Szabo G, Molnar Z, Paulsen O (2004) Preferential origin and layer destination of GAD65-GFP cortical interneurons. Cereb Cortex 14: 1122-1133.

25. Lujan R, Nusser Z, Roberts JD, Shigemoto R, Somogyi P (1996) Perisynaptic location of metabotropic glutamate receptors mGluR1 and mGluR5 on dendrites and dendritic spines in the rat hippocampus. Eur J Neurosci 8: 1488-1500.

26. Mannaioni G, Attucci S, Missanelli A, Pellicciari R, Corradetti R, Moroni F (1999) Biochemical and electrophysiological studies on (S)-(+)-2-(3 '-carboxybicyclo[1.1.1]pentyl)-glycine (CBPG), a novel mGlu(5) receptor agonist endowed with mGlu(1) receptor antagonist activity. Neuropharmacology 38: 917-926.

27. Maccaferri G, Tóth K, McBain CJ. (1998). Target-specific expression of presynaptic mossy fiber plasticity. Science. 279:1368-70.

28. McBain CJ, DiChiara TJ, Kauer JA. (1994) Activation of metabotropic glutamate receptors differentially affects two classes of hippocampal interneurons and potentiates excitatory synaptic transmission. J Neurosci. 14:4433-45.

29. McBain CJ, Fisahn A (2001) Interneurons unbound. Nat Rev Neurosci 2: 11-23.

30. Munoz A, Liu XB, Jones EG (1999) Development of metabotropic glutamate receptors from trigeminal nuclei to barrel cortex in postnatal mouse. J Comp Neurol 409: 549-566.

31. Nakajima Y, Iwakabe H, Akazawa C, Nawa H, Shigemoto R, Mizuno N, Nakanishi S (1993) Molecular characterization of a novel retinal metabotropic glutamate receptor mGluR6 with a high agonist selectivity for L-2-amino-4-phosphonobutyrate. J Biol Chem 268: 11868-11873.

32. Pelkey KA, Lavezzari G, Racca C, Roche KW, McBain CJ (2005) mGluR7 is a metaplastic switch controlling bidirectional plasticity of feedforward inhibition. Neuron 46: 89-102.

33. Petralia RS, Wang YX, Singh S, Wu C, Shi L, Wei J, Wenthold RJ (1997) A monoclonal antibody shows discrete cellular and subcellular localizations of mGluR1 alpha metabotropic glutamate receptors. J Chem Neuroanat 13: 77-93.

34. Pin JP, Waeber C, Prezeau L, Bockaert J, Heinemann SF (1992) Alternative splicing generates metabotropic glutamate receptors inducing different patterns of calcium release in Xenopus oocytes. Proc Natl Acad Sci U S A 89: 10331-10335.

35. Salt TE. (2002) Glutamate receptor functions in sensory relay in the thalamus. Philos Trans R Soc Lond B Biol Sci. 357:1759-66.

36. Sandstrom MI, Rebec GV. (2007) Extracellular ascorbate modulates glutamate dynamics: role of behavioral activation. BMC Neurosci. 8:32.

37. Sekizawa S, Bonham AC. (2006) Group I metabotropic glutamate receptors on second-order baroreceptor neurons are tonically activated and induce a Na+-Ca2+ exchange current. J Neurophysiol. 95: 882-92.

38. Schoepp et al (1999) Pharmacological agents acting at subtypes of metabotropic glutamate receptors. Neuropharmacology 38 1431.

39. Sun QQ, Huguenard JR, Prince DA (2006) Barrel cortex microcircuits: thalamocortical feedforward inhibition in spiny stellate cells is mediated by a small number of fast-spiking interneurons. J Neurosci 26: 1219-1230.

40. Tamamaki N, Yanagawa Y, Tomioka R, Miyazaki JI, Obata K, Kaneko T (2003) Green fluorescent protein expression and colocalization with calretinin, parvalbumin, and somatostatin in the GAD67-GFP knock-in mouse. Journal of Comparative Neurology 467: 60-79.

41. Tóth K, McBain CJ. Target-specific expression of pre- and postsynaptic mechanisms. J Physiol. 2000 May 15;525 Pt 1:41-51.

42. Wang Y, Gupta A, Toledo-Rodriguez M, Wu CZ, Markram H (2002) Anatomical, physiological, molecular and circuit properties of nest basket cells in the developing somatosensory cortex. Cereb Cortex 12: 395-410.

43. Wong RK, Chuang SC, Bianchi R (2004) Plasticity mechanisms underlying mGluR-induced epileptogenesis. Adv Exp Med Biol 548: 69-75.

44. Young A, Sun QQ (2007) Long-Term Modifications in the Strength of Excitatory Associative Inputs in the Piriform Cortex. Chem Senses.

45. Zhang C, Szabo G, Erdelyi F, Rose JD, Sun QQ (2006) Novel interneuronal network in the mouse posterior piriform cortex. J Comp Neurol 499: 1000-1015.

Figure legend

Figure 1. GAD65-GFP and GAD67-GFP interneurons in barrel cortex layer 4.
A) Photomicrograph of barrel cortex brain slice layer 4 region showing that none of the GAD65-GFP-positive interneurons (A1) express parvalbumin (A2). In A3, GFP cells (green) and PV cells (red) are not colocalized. White arrowheads indicate three GAD65-GFP positive cells. None of these cells express PV. ***B)*** Photomicrograph of barrel cortex brain slice layer 4 showing that majority of the GAD67-GFP-positive interneurons (B1) in the barrel overlap with the parvalbumin-positive interneurons (B2). Note that majority of GFP cells (green) are colocalized with PV cells (red), because majority of cells in B3 barrel are yellow. Dashed lines in A & B demarcate barrels layer 4. Scale bar in B &A: 50 μm. ***C)*** Firing properties of RSNP vs. FS cells. The instant frequency of repetitive spikes induced 150pA (open circles) and 250 pA current injection (filled circles) in a RSNP (***C1***) and FS (***C2***) cell. Solid lines: single exponential decay fitting curves. ***D)***: Current clamp recording from a RSNP (D1) and FS (D2) cell showing the firing pattern of each cell. ***E***) In the GAD67-GFP mice, whole-cell patch-clamp recording results show that 82±5% GFP-positive cells (n=30) show FS firing pattern. In contrast, none of the GAD65-GFP cells (n=40) exhibited FS firing pattern ($p<0.001$, ***E1***). This is consistent with the percentage of cells expressing PV in GAD67-GFP vs. GAD65-GFP cells (***E2*)**. Inset: Firing pattern of a representative RSNP (top, a GAD65-GFP cell) and FS (bottom, a GAD67-GFP cell) cell, respectively. ***:$p<0.001$.

Figure 2. Two distinct inhibitory interneuron types in barrel cortex layer 4. The figure shows differences in morphological properties of RSNP vs. FS cells. ***A1&B1)*** Camera lucida reconstruction of intracellularly labeled RSNP and GAD65-GFP (***A1***) and GAD67-GFP and FS (***B1***) cells in the barrel cortex. Blue: dendrites and somata; Red: axons; gray shading: barrel structure which was identified via cytochrome C staining in an adjacent section (60 μm in thickness). Scale bar near interneuron: 20 μm. Inset near each of the interneuron: spikes induced by intracellular current injection (200 pA). ***A2***& ***B2)*** Sholl analysis showing radium distribution of axons of the RSNP (black) and FS cell (red). ***A3*** &***B3)*** Polar histogram showing distribution of axons of the RSNP (black) and FS cell (red). Orientation of polar histogram and the radial scale are shown in the figure. From this figure, it is clear that dendritic and axonal arborizations of RSNP and FS cells has different patterns (i.e. angular orientation, densities).

Figure 3. Immunohistochemical images of mGluR receptors in GAD65-GFP (RSNP) cells. ***A1&B1***): Digitally enhanced micrographs of GAD65-GFP positive interneurons in layer IV barrel cortex. ***A2&B2***): Immunofluorescent images of the same sections above, showing mGluR2/3(***A2***) and mGluR5 (***B2***) in neocortical interneurons. Scale bars=10 μm. Dotted red lines demarcate the perikaryon and primary dendrites of the GFP-positive interneurons. Insets: triple labeled photomicrograph of GAD65-GFP cells (green), PV-IR (blue) and mGluR2/3-IR (red, A2) or mGluR5-IR (red, B2). Scale bars=25 μm. Arrowheads; GFP positive (black arrowheads), or PV-positive cells (white arrowheads). Note that in both A2&B2, expression levels of mGluRs were higher in GAD65-GFP positive cells than PV-positive cells. ***C)*** Pooled data showing the comparison of gray scale fluorescent intensities of mGluR-IRs in GAD65-gfp positive cells vs. PV-positive cells the same optical section in GAD65-GFP mice. **: $p<0.01$, *:$p<0.05$, n=5 sections from two perfused brains.

Figure 4. Immunohistochemical images of mGluR receptors in GAD67-GFP cells. ***A1-C1***): Digitally enhanced micrographs of GAD67-GFP positive interneurons

in layer IV barrel cortex. ***A2-C2***): Immunofluorescent images of the same sections above, showing mGluR1(***A2***), mGluR5 (***B2***) and mGluR8 (***B2***) in GAD67-GFP cells. Scale bars=10 μm. Dotted red lines demarcate the perikaryon of the GFP-positive interneurons. Inserts inB2 & C2 showing colocalization of mGluR 8-IR (red) but not mGluR5-IR in PV (blue) positive cells. Dotted red lines demarcate the perikaryon of the PV-positive interneurons. Scale bars=4 μm. ***D)*** Triple labeled photomicrograph of GAD67-GFP cells (green), PV-IR (blue) and mGluR1-IR (red, D1), mGluR5-IR (red, D2) and mGluR8-IR (red, D3). Scale bars=5 μm. White small arrowheads: mGluR positive puncta near soma. Large arrowheads: mGluR positive puncta in dendrites. ***E)*** Pooled data showing the comparison of gray scale fluorescent intensities of mGluR-IRs in PV-positive vs. PV-negative cells (all cells are GFP positive) in the same optical section in GAD67-GFP mice. **: $p<0.01$, *:$p<0.05$, n=6 sections from two perfused brains.

Figure 5. Effects of mGluR5 agonist CHPG on mEPSCs in RSNP vs. FS cells. ***A1)*** Patch clamp recording from a GAD65-GFP positive interneuron visualized under DIC microscopy. White arrowhead: patch-clamp recording pipette. White colored trace: action potentials (RSNP type) induced in this cell. Inset: image of the same cell visualized under epifluorescent mode. Scale bar: 10 μm. ***B1)*** Patch clamp recording from a GAD67-GFP positive interneuron visualized under DIC (insert) and fluorescent microscopy. White arrowhead in insert: recording pipette. White colored trace in the insert: action potentials (FS-type) induced in this cell. Scale bar: 10 μm. ***A2 & B2)*** mEPSCs recorded in the RSNP (A2) and FS (B2) cells in the absence (control and washout) and presence of CHPG (1 mM). Gray solid lines marks the baseline (center) and noise level (top and bottom). ***A3 &B3)*** Averaged mEPSCs of the recordings of A2&B2, respectively. The time scale of the EPSCs was expanded to show single AMPA mediated EPSC. ***C)***: Effects of CHPG (1 mM) on frequency and amplitudes of mEPSCs in RSNP (n=6) and FS cells (n=6).

Figure 6. Effects of mGluR5 agonist CHPG on evoked EPSCs and holding currents in RSNP vs. FS cells. ***A1&B1)*** Representative traces of evoked EPSCs

in control condition (a), in the presence of CHPG (b) and after washout (c) in a RSNP (***A1***) and FS cell (***B1***). ***A2&B2)*** Time series measurements of eEPSCs (filled circles) and holding currents (open circles) in an experiment of CHPG application (filled gray bars). Solid gray line: running average. Dotted line: baseline recording level based on running average of control and washout data. ***A3&B3)*** Time series measurements of paired pulse ratio (PPR) of the eEPSCs (eEPSC2/eEPSC1, filled circles) of the same experiment of A2 &B2. Inserts: Normalized eEPSCs before (a), after (c, gray trace) and during application of CHPG (b). Dotted line: baseline recording level based on running average of control and washout data. ***C)*** Pooled data showing the effects of CHPG on amplitude of eEPSCs (***C1***), PPR (***C2***) and holding currents (***C3***) in RSNP (n=6) vs. FS (n=6) cells. **: $p<0.01$; *$p<0.05$, One-Way Anova.

Figure 7. Effects of L-AP4 in RSNP vs. FS cells. ***A1&B1)*** Representative traces of evoked EPSCs in control condition (a), in the presence of L-AP4 (b) and after washout (c) in a RSNP (***A1***) and FS cell (***B1***). Inserts: normalized eEPSCs before (a), after (c, gray trace) and during application of L-AP4 (b). ***A2&B2)*** Representative traces of eEPSCs evoked by two pulses (to show PPR) in control condition (a), in the presence of L-AP4 (b) and after washout (c) in a RSNP (***A2***) and FS cell (***B2***). Inset: Membrane responses recorded in absence (control and washout) and presence of l-AP4 (gray trace).It is clear that L-AP4 had no effect on conductance. ***C)*** sEPSCs recorded in a RSNP cell (***C1***) and a FS cell (***C2***) in the absence (control and washout) and presence of L-AP4(100 μM). * marks a event (i.e. single EPSC) recognized by automated event detection program. Dashed lines mark the baseline (center) and noise level (top and bottom). Pooled data showing the effects of L-AP4 on the amplitude (***C3***) and frequency (***C4***) of sEPSCs in RSNP (n=9) and FS (n=8) cells. *:$p<0.05$. ***D)*** Pooled data showing the effects of L-AP4 on the amplitude of eEPSCs (***D1***) and PPR (***D2***) in RSNP (n=9) vs. FS (n=8) cells. **: $p<0.01$; ***:$p<0.001$.

Figure 8. mGluR agonists induced effects on eEPSCs in RSNP and FS cells. ***A1 &A2)*** Representative traces of evoked EPSCs in control condition (a), in the presence of L-AP4 alone (b), in the presence of L-AP4+CHPG (c) and after washout (d) in a RSNP (***A1***) and FS cell (***B1***). Inserts: normalized eEPSCs before (a), after (d, gray trace) and during application of agonist (b &c). ***B)*** Pooled data of the experiments of A showing the effects of L-AP4 alone and L-AP4+ CHPG in FS and RSNP neurons (n=5-9 in each group). ***C)*** The effects of all mGluR agonists on the eEPSCs amplitude (***C1***) and holding currents (***C2***) in RSNP cells and FS cells (n=6-31 in each group). **: p<0.01, *:p<0.05.

Figure 9. Effects of mGluR agonists on the intrinsic excitabilities of FS and RSNP cells. A1) Effects of (±)-trans-ACPD (100 μM, gray bar) on action potentials induced direct current injection and synaptic stimulation. ***A2)*** Representative traces in absence (black trace, a) and presence of (±)-trans-ACPD (gray trace, b). The spikes were induced with a short step of current injection (200pA, 2 ms) followed by electrically stimulation in an adjacent cortical area (two pulses at an interval of 5 ms). ***B1)*** Effects of (±)-trans-ACPD (100 μM) on conductance of RSNP (open bar, n=23) and FS cells (black bar, n=31). ***B2)*** The effects of mGluR agonists and antagonists on the conductance of FS cells. **:p<0.01, One-way Anova, n=6-31 in different groups.

Supplemental results.

mGluR differentially regulate excitatory synaptic transmission and intrinsic membrane conductance in RSNP vs. FS interneurons. We examined the effects of mGluR group I and II agonist, (±)-trans-ACPD (100 μM), on miniature (in the presence of TTX and picrotoxin) EPSCs (mEPSCs) in RSNP and FS cells (supplemental Fig 1). Our results showed that in the presence of (±)-trans-ACPD, both the amplitudes (58±6%, n=6; p<0.01) and frequency (36±8%, n=6, p<0.05) of

the mEPSCs were significantly reduced in RSNP but not in FS cell (n=9) groups (supplemental Fig 1A vs. B). These results suggest that both presynaptic and postsynaptic mechanisms may be involved. However, postsynaptic mechanism could be more prominent, because at very negative holding potentials (-100 mV), the reduction in frequency of mEPSCs reduced to 10±3% (p=0.1 vs. controls, n=6).

We next examined the effects of (±)-trans-ACPD (100 μM) on electrically evoked EPSCs in RSNP vs. FS cells (supplemental Fig 2). In cells with RSNP firing properties, local perfusion of (±)-trans-ACPD (100 μM) induced rapid and reversible inhibition of eEPSCs (supplemental Fig 2A, 55±4% inhibition; n=23, p<0.001 vs. controls). In the majority of FS cells, (±)-trans-ACPD, at the same concentration, had very little effect on the eEPSCs in 25/31 FS cells (e.g. supplemental Fig 1B, 15±8%, p>0.1, n=31) but instead, induced robust inhibition of holding currents in 27/31 cells (e.g. Fig. 9B1&2). In the majority (19/23) of RSNP cells, there was no significant effect of ACPD on the intrinsic conductance which was measured simultaneously with synaptic potentials under voltage clamp (cf. supplemental Fig 2A; n=23, p>0.1). On average, the (±)-trans-ACPD induced conductance is 1.1±0.1 nS in FS cells but only 0.2±0.0 nS in RSNP cells (Fig 9, p<0.01 RSNP vs. FS). In current clamp mode, (±)-trans-ACPD induced robust depolarization and enhanced spontaneous firing in the FS cells (7±2 mv, n=10; e.g. Fig. 5) but not in RSNP cells (3±2 mV, n=10). Thus group I/ II mGluR receptor agonist (±)-trans-ACPD mediated inhibition of glutamate transmission in RSNP cells but not in FS cells (supplemental Fig 1), and induced rapid depolarization in FS cells but not in RSNP cells (Fig 9). We also monitored the paired-pulse ratio before, during and after the application of (±)-trans-ACPD. Despite

the robust inhibition of the amplitude of eEPSCs in RSNP cells, the paired-pulse ratio of eEPSCs remained largely unchanged throughout the experiments (supplemental Fig 2A3 &6A). These results are consistent with the effects of ACPD on mEPSCs in RSNP cells and indicated that a postsynaptic mechanism mediated the effects in RSNP cells.

FS interneurons can be further divided into morphologically distinct groups (large basket cells vs. small basket cells,(Wang et al., 2002)), where they all express the calcium binding protein, parvalbumin (Fig. 1) and belong to the basket cell category (Wang et al., 2002). In 10% (3 cells) FS cells, in addition to a robust effect on membrane depolarization, trans-ACPD had small effects on glutamate transmission. This suggests that heterogeneity may exist within the FS group, as demonstrated by previous studies. However, other than showing synaptic modulation to mGluR in of the three cells, we could not find any other differences (e.g. firing pattern or expression of mGluRs) within the majority of the FS cells (90%).

Legend

Supplemental Figure 1. Effects of GROUP I &II mGluR agonist (±)-trans-ACPD on mEPSCs in RSNP vs. FS cells. ***A1 & B1)*** mEPSCs recorded in the RSNP (A2) and FS (B2) cells in the absence (control and washout) and presence of (±)-trans-ACPD (100 μM). * marks a event (i.e. single EPSC) recognized by automated event detection program. Gray dashed lines marks the baseline (center) and noise level (top and bottom). ***A2-B3)***: Effects of (±)-trans-ACPD (100 μM) on frequency and amplitudes of mEPSCs in RSNP (n=6) and FS cells (n=9).

Supplemental Figure 2. Effects of mGluR agonist (±)-trans-ACPD on evoked EPSCs and holding currents in RSNP vs. FS cells. ***A1&B1)*** Representative traces of evoked EPSCs in control condition (a), in the presence of(±)-trans-ACPD (b) and after washout (c) in a RSNP (***A1***) and FS cell (***B1***). ***A2&B2)*** Time series measurements of eEPSCs (filled circles) and holding currents (open circles) in an experiment of (±)-trans-ACPD application (filled gray bars). Solid gray line: running average. Insert in A2: no effects of trans-ACPD (b) on intrinsically induced membrane responses. ***A3&B3)*** Time series measurements of paired pulse ratio of the eEPSCs (eEPSC2/eEPSC1, filled circles) of the same experiment of A2 &B2. Inserts on the right: representative evoked EPSCs before (a), after (c, gray trace) and during application of ACPD (b). ***C)*** Pooled data showing the effects of trans-ACPD on amplitude of eEPSCs (***C1***) and holding currents (***C2***) in RSNP (n=23) vs. FS (n=31) cells. **: $p<0.01$; *$p<0.05$, One-Way Anova.

Supplemental Figure 3. Effects of mGluR5 agonist CHPG on sEPSCs in RSNP vs. FS cells. A1 & B1) sEPSCs recorded in the RSNP (A1) and FS (B1) cells in the absence (control and washout) and presence of CHPG (1 mM). * marks a event (i.e. single EPSC) recognized by automated event detection program. Gray dashed lines marks the baseline (center) and noise level (top and bottom). A2 &B2) Averaged EPSCs of the recordings of A1&B1, respectively. The time scale of the EPSCs was expanded to show single AMPA mediated EPSC. C): Effects of CHPG (1 mM) on frequency and amplitudes of mEPSCs in RSNP (n=7) and FS cells (n=8).

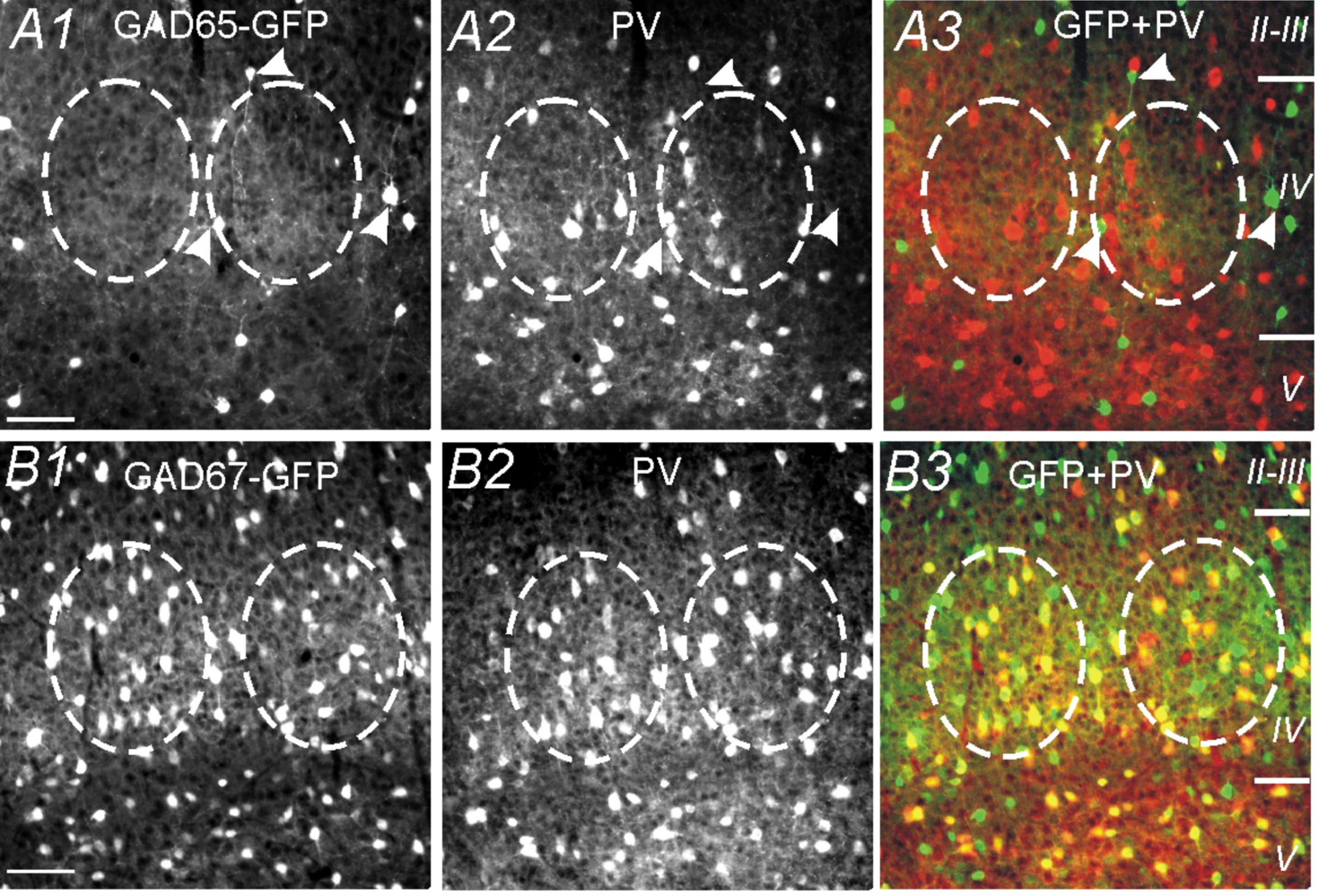
A1
GAD65-GFP
A2
PV
A3
GFP+PV
II-III
IV
V
B1
GAD67-GFP
B2
PV
B3
GFP+PV
II-III
IV
V

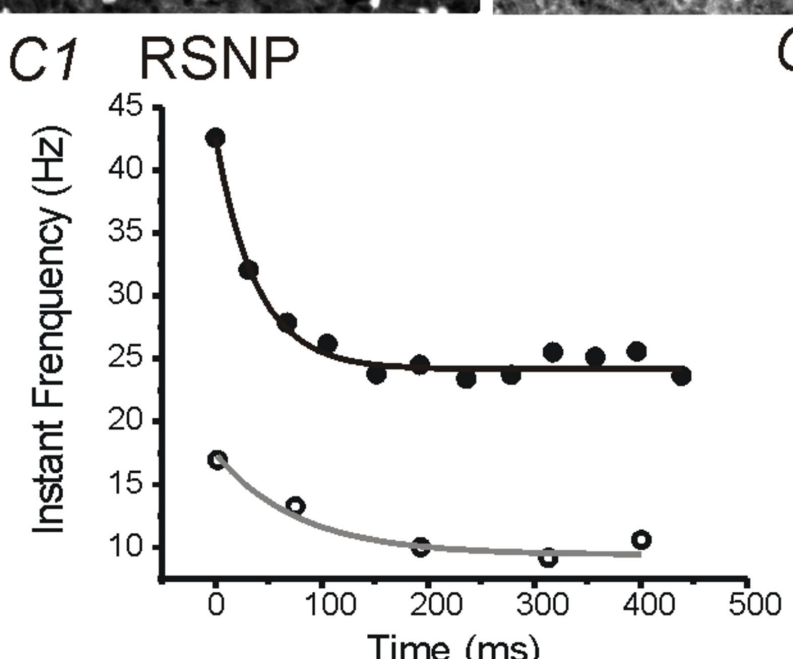
C1
RSNP
Instant Frenquency (Hz)
45
40
35
30
25
20
15
10
0
100
200
300
400
500
Time (ms)

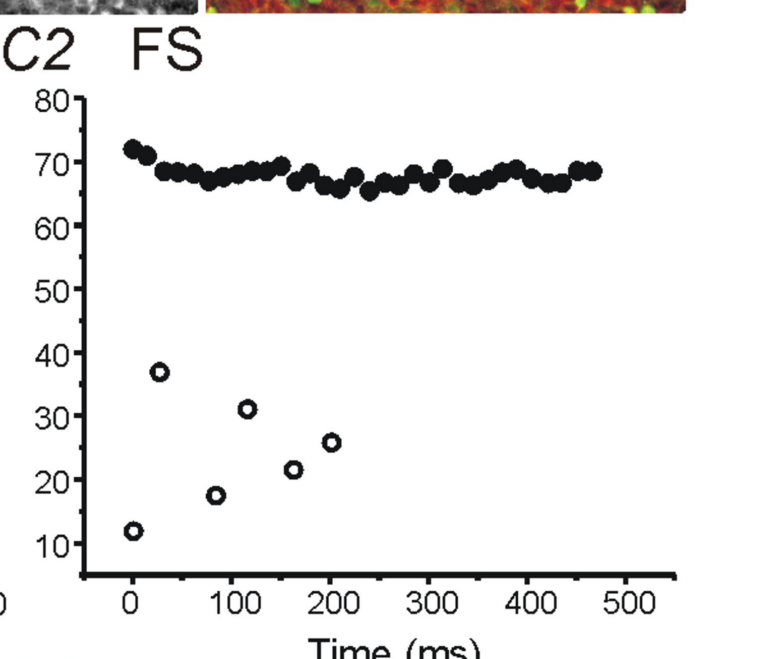
C2
FS
80
70
60
50
40
30
20
10
0
100
200
300
400
500
Time (ms)

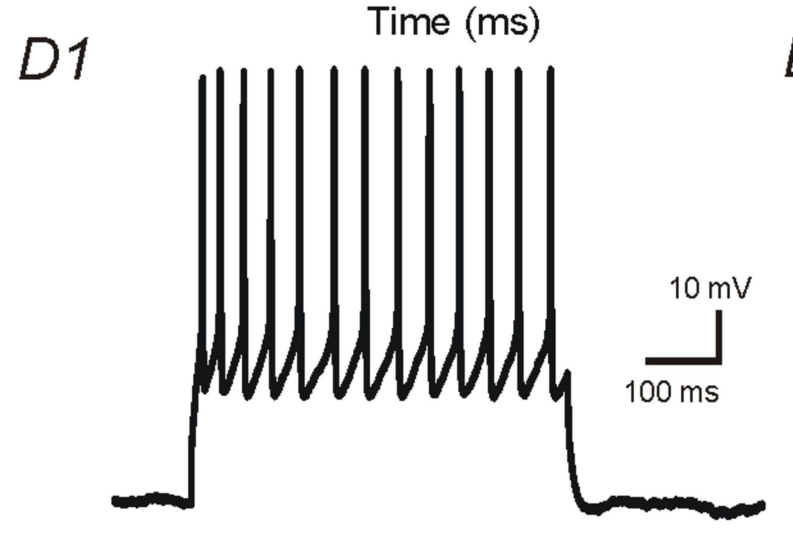
D1
10 mV
100 ms

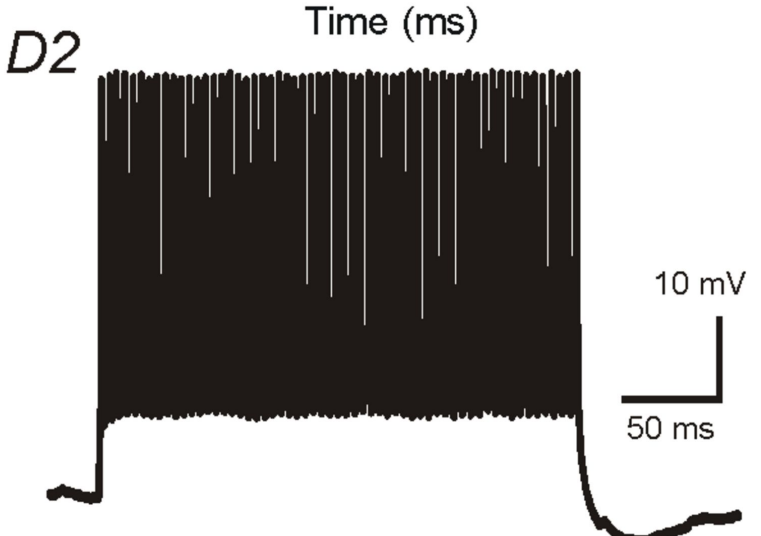
D2
10 mV
50 ms

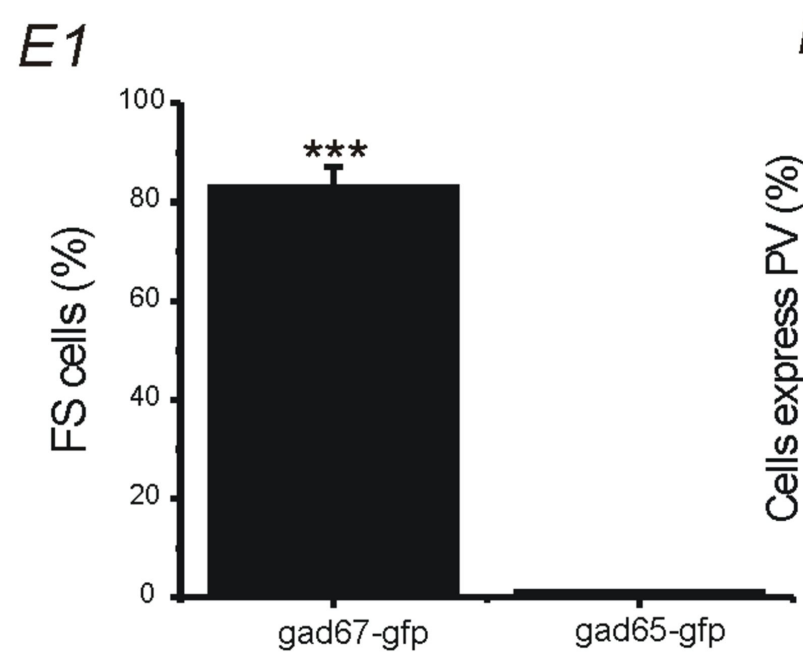
E1
FS cells (%)
100
80
60
40
20
0
***
gad67-gfp
gad65-gfp

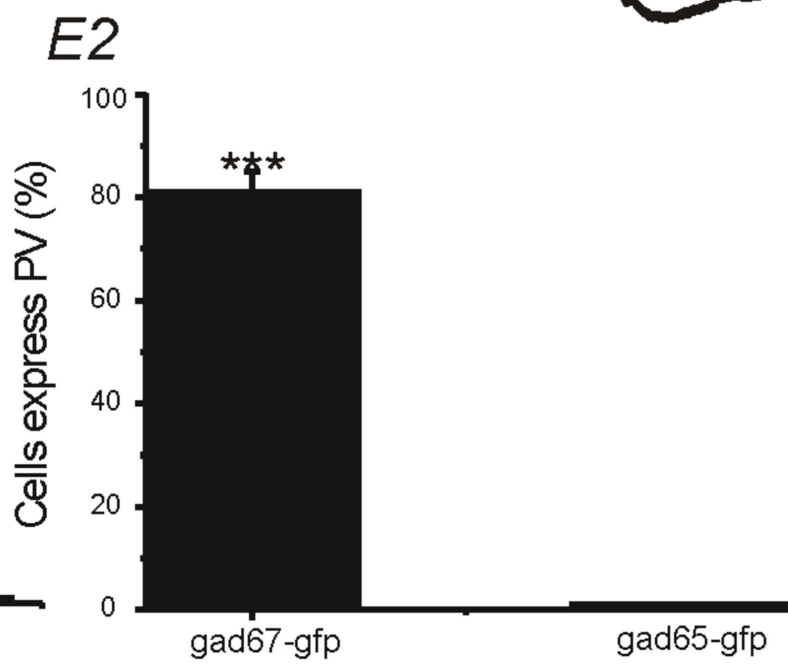
E2
Cells express PV (%)
100
80
60
40
20
0
***
gad67-gfp
gad65-gfp

Fig 1

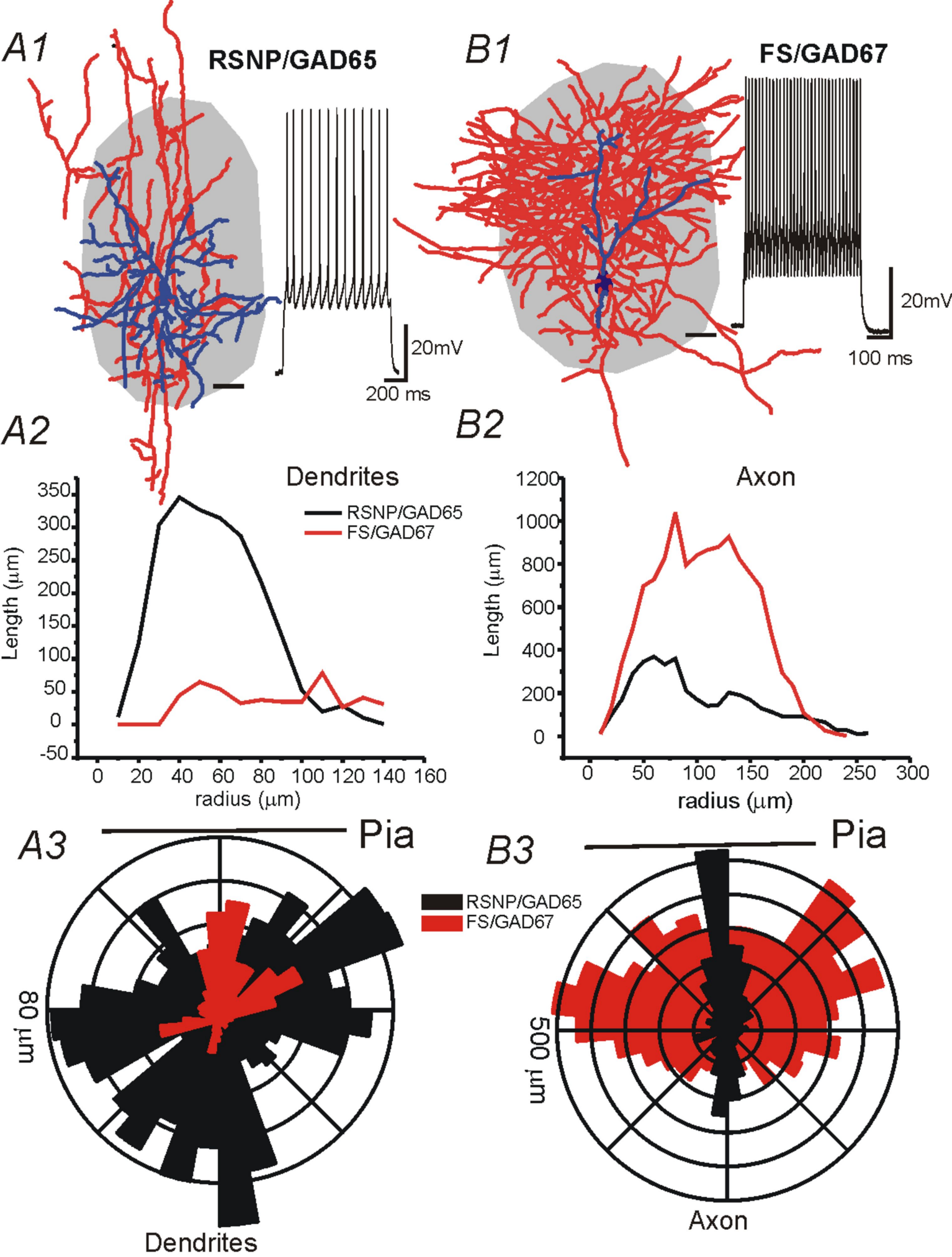
A1
RSNP/GAD65
20mV
200 ms
B1
FS/GAD67
20mV
100 ms
A2
Dendrites
RSNP/GAD65
FS/GAD67
Length (μm)
radius (μm)
B2
Axon
Length (μm)
radius (μm)
A3
Pia
80 μm
Dendrites
B3
Pia
RSNP/GAD65
FS/GAD67
500 μm
Axon

Fig 2

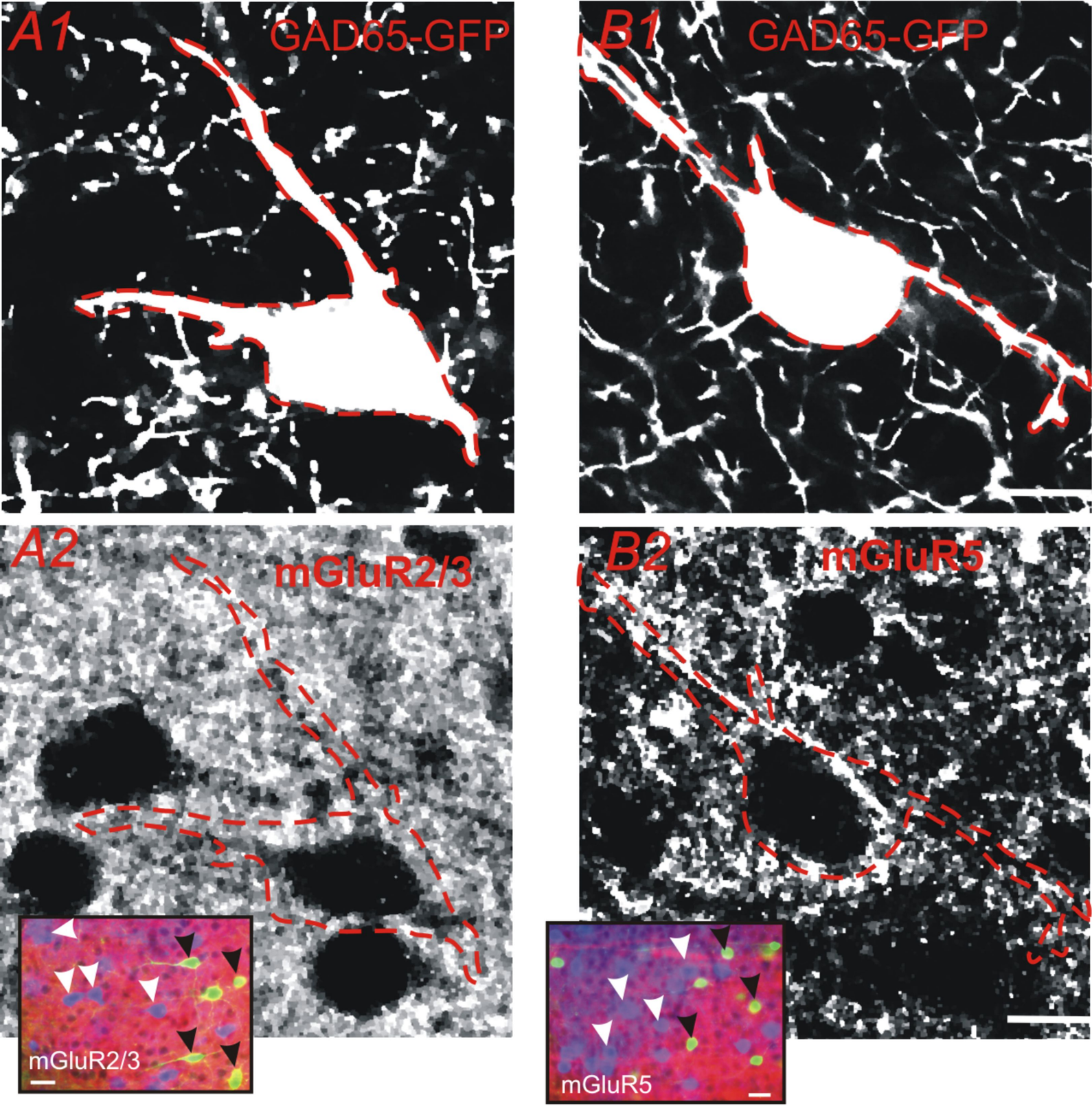
A1
GAD65-GFP
B1
GAD65-GFP
A2
mGluR2/3
B2
mGluR5
mGluR2/3
mGluR5

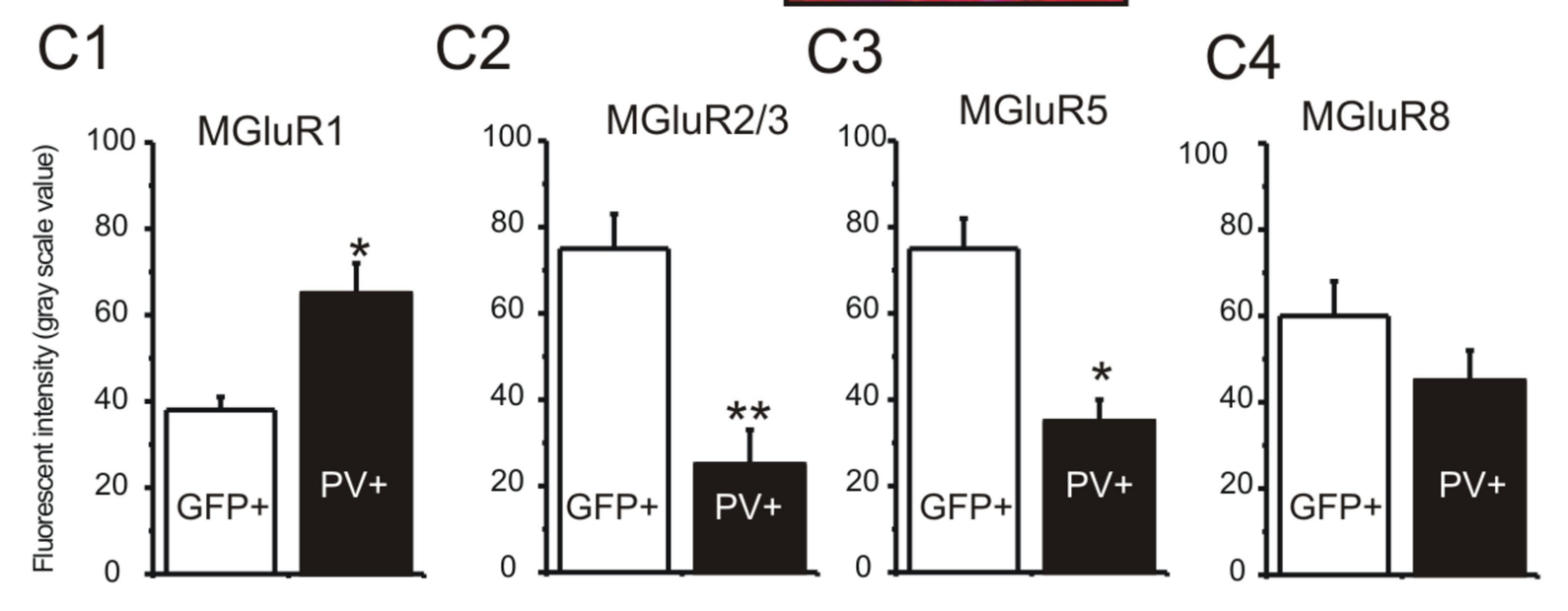
C1
MGluR1
C2
MGluR2/3
C3
MGluR5
C4
MGluR8
Fluorescent intensity (gray scale value)
100
80
60
40
20
0
GFP+
PV+
*
**
*

Fig. 3

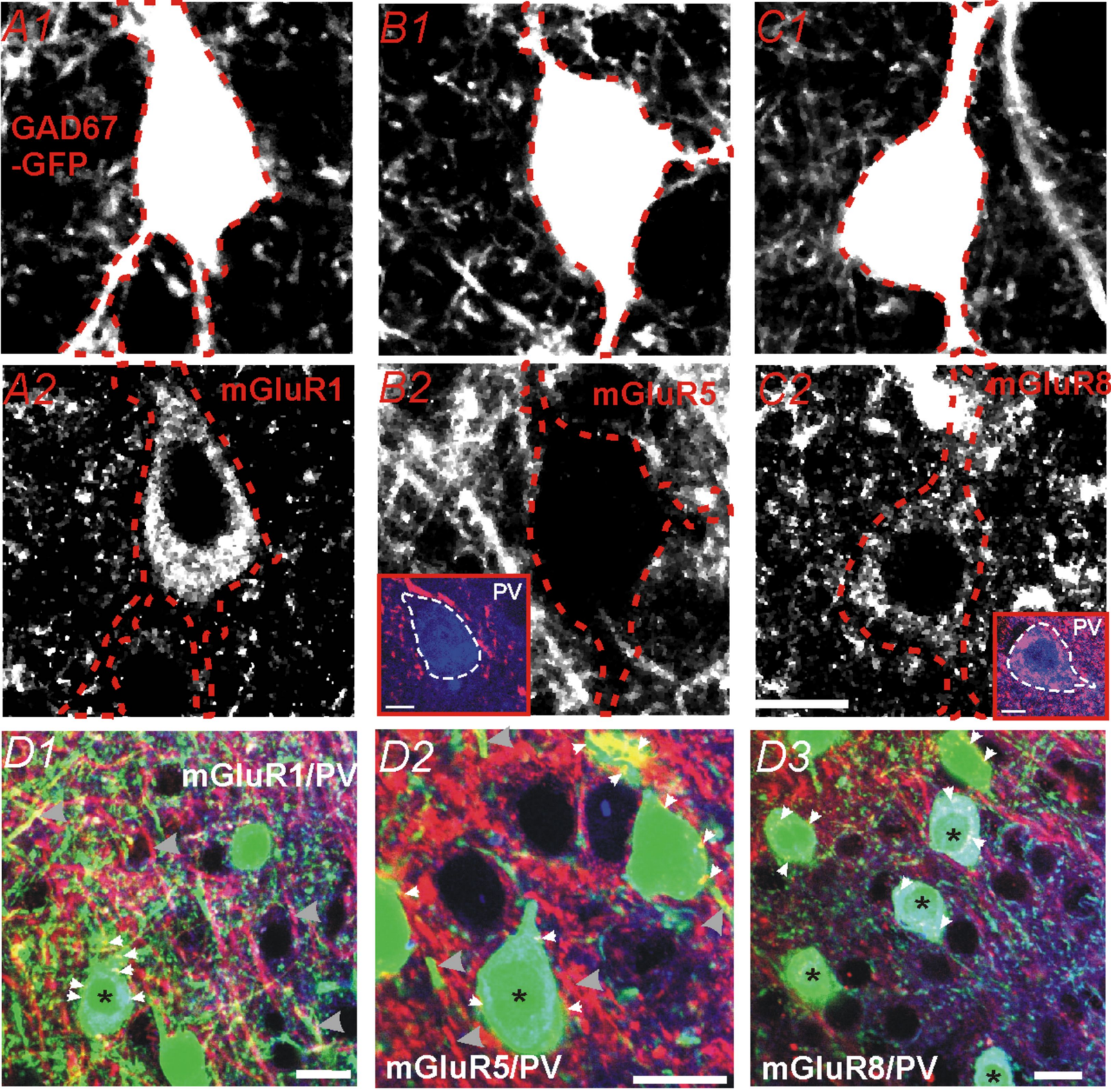
A1
GAD67
-GFP
B1
C1
A2
mGluR1
B2
mGluR5
PV
C2
mGluR8
PV
D1
mGluR1/PV
D2
mGluR5/PV
D3
mGluR8/PV

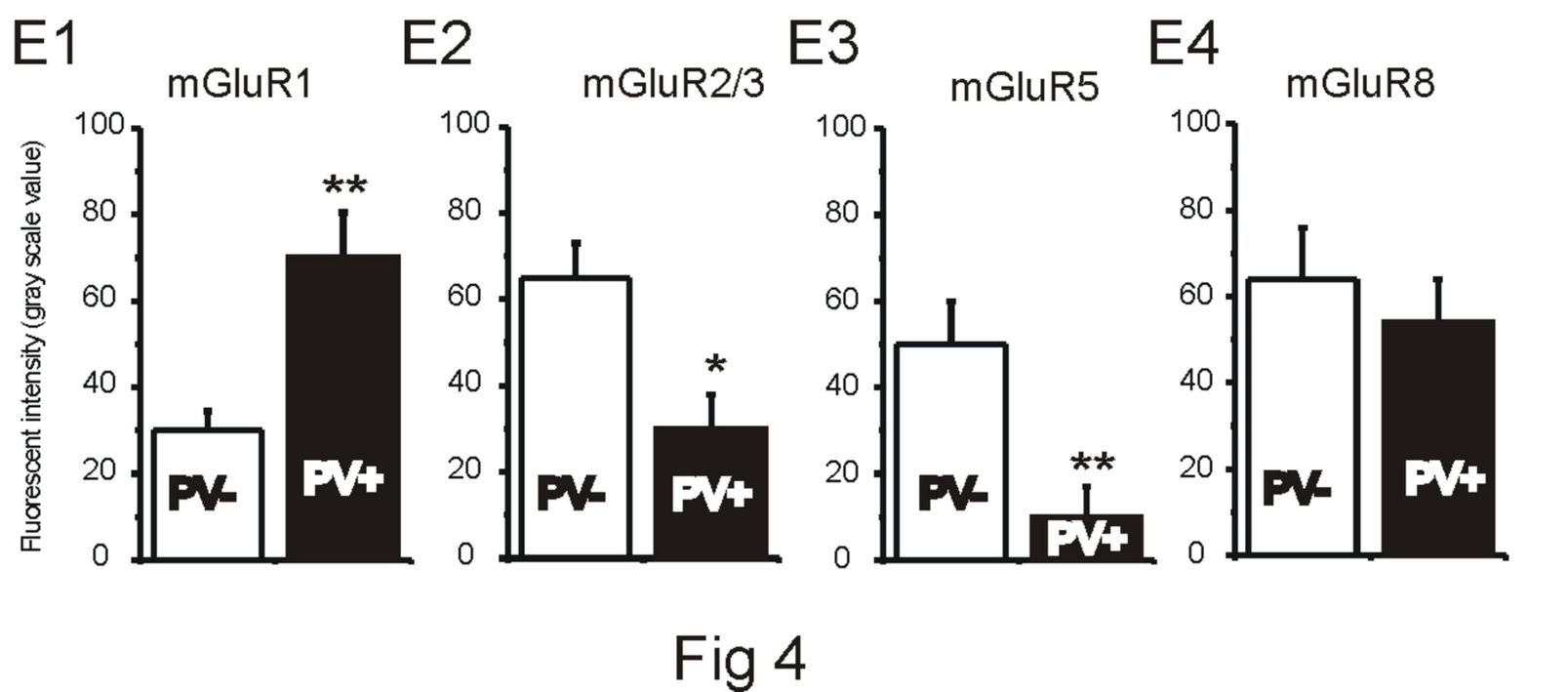
E1
mGluR1
E2
mGluR2/3
E3
mGluR5
E4
mGluR8
Fluorescent intensity (gray scale value)
100
80
60
40
20
0
**
*
**
PV-
PV+

Fig 4

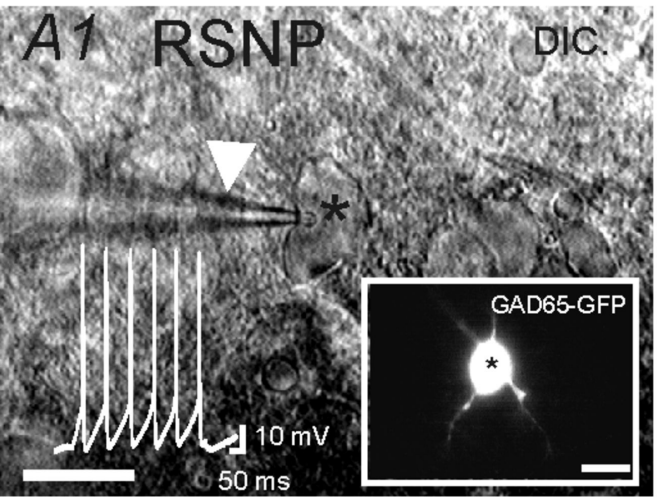
A1 RSNP
DIC.
GAD65-GFP
10 mV
50 ms

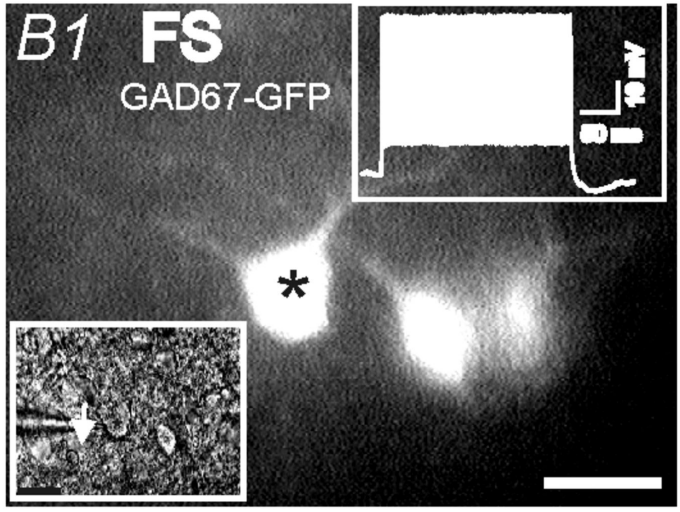
B1 FS
GAD67-GFP

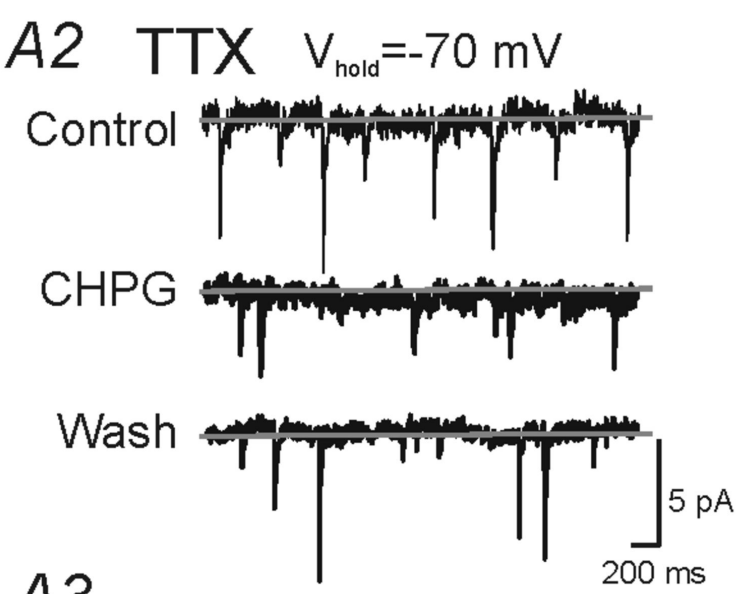
A2 TTX V_{hold}=-70 mV
Control
CHPG
Wash
5 pA
200 ms

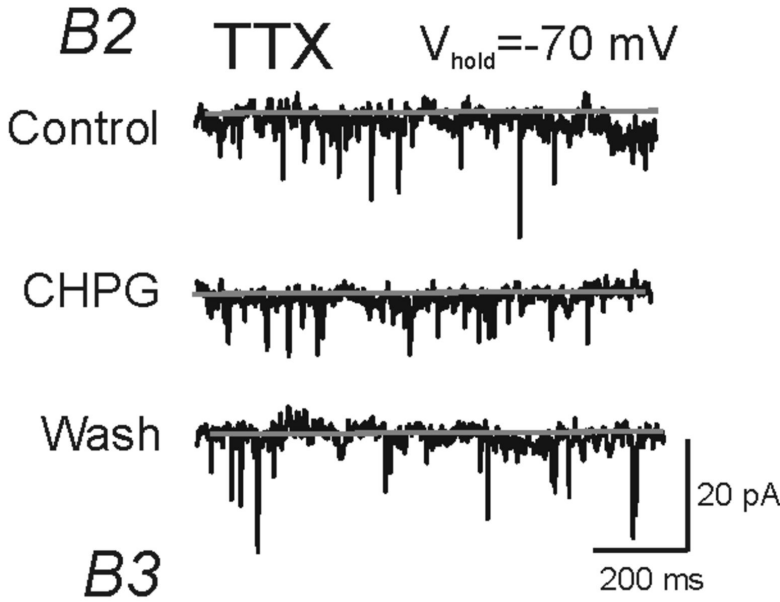
B2 TTX V_{hold}=-70 mV
Control
CHPG
Wash
20 pA
200 ms

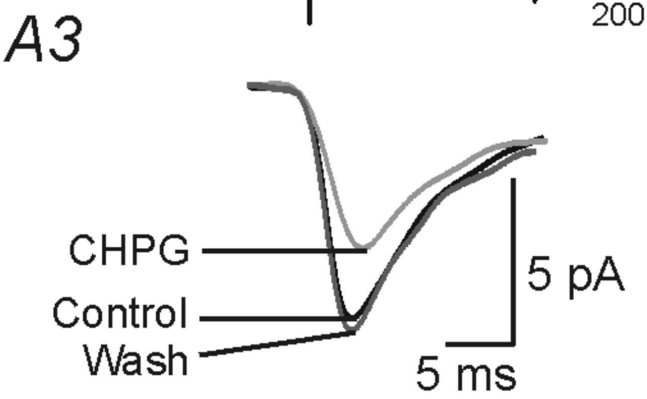
A3
CHPG
Control
Wash
5 pA
5 ms

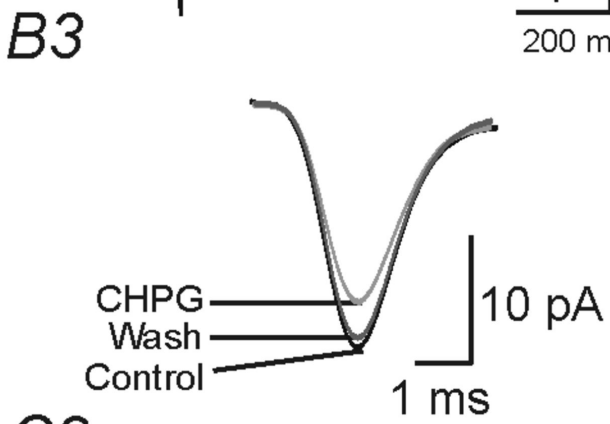
B3
CHPG
Wash
Control
10 pA
1 ms

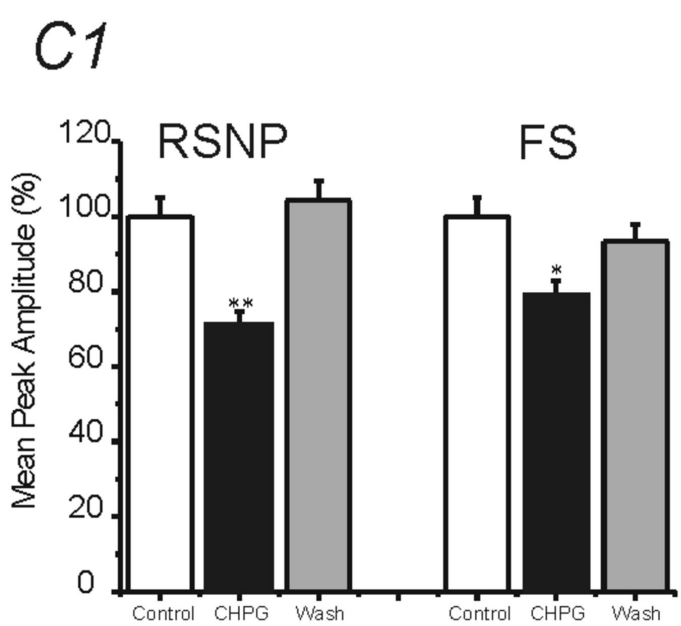
C1
RSNP
FS
Mean Peak Amplitude (%)
120
100
80
60
40
20
0
**
*
Control
CHPG
Wash
Control
CHPG
Wash

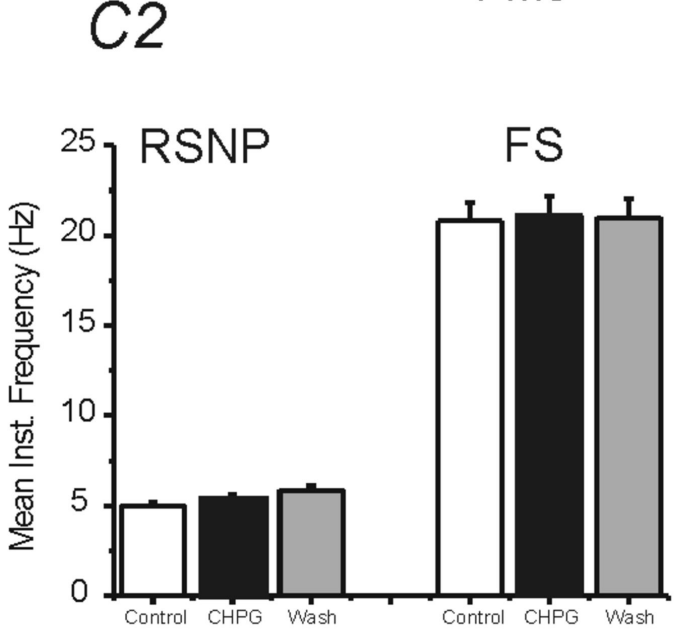
C2
RSNP
FS
Mean Inst. Frequency (Hz)
25
20
15
10
5
0
Control
CHPG
Wash
Control
CHPG
Wash

Fig 5.

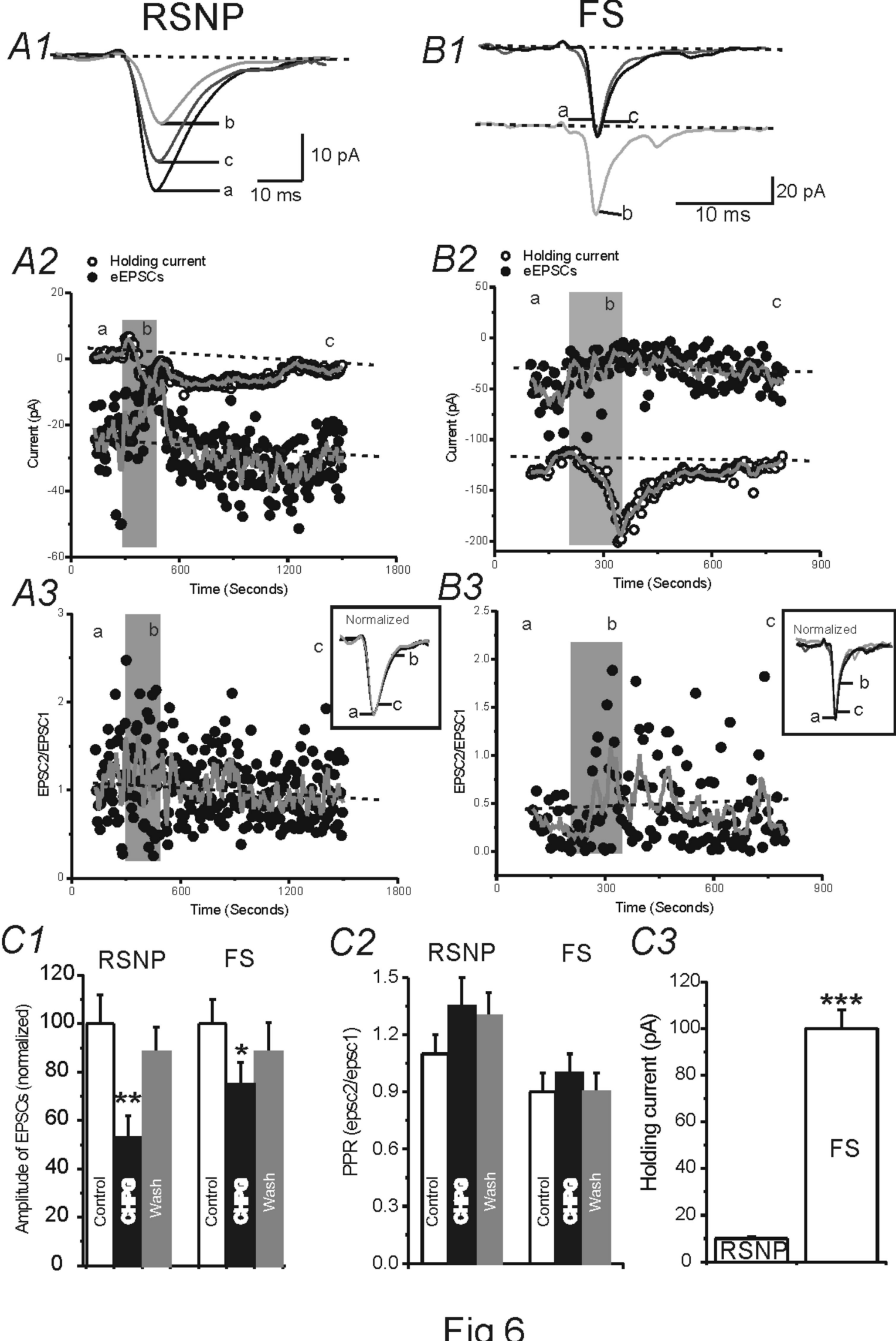
RSNP
FS
A1
B1
b
c
a
10 pA
10 ms
20 pA
A2
B2
Holding current
eEPSCs
Current (pA)
Time (Seconds)
A3
B3
EPSC2/EPSC1
Normalized
C1
C2
C3
Amplitude of EPSCs (normalized)
PPR (epsc2/epsc1)
Holding current (pA)
Control
CPP
Wash
RSNP
FS
**
*
***

Fig 6

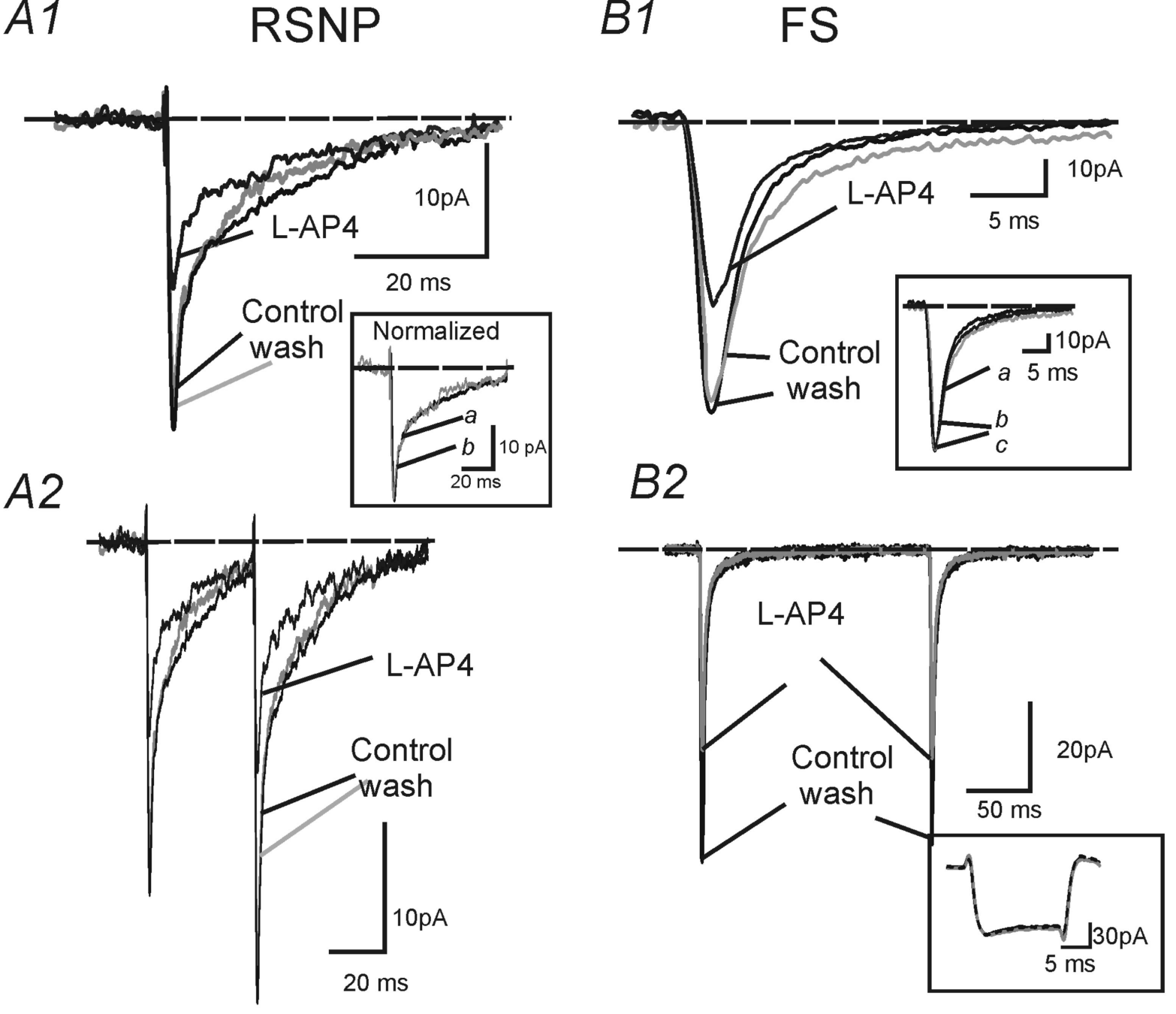
A1
RSNP
10pA
L-AP4
20 ms
Control
wash
Normalized
a
b
10 pA
20 ms
B1
FS
L-AP4
10pA
5 ms
Control
wash
a
b
c
10pA
5 ms
A2
L-AP4
Control
wash
10pA
20 ms
B2
L-AP4
Control
wash
20pA
50 ms
30pA
5 ms
C1
RSNP
Control
L-AP4
Washout
2 pA
200 ms
C2
FS
Control
L-AP4
Washout
4pA
20 ms
C3
RSNP
FS
Amplitude of EPSCs (normalized)
120
100
80
60
40
20
0
Control
L-AP4
Wash
*
C4
RSNP
FS
Frequency (Hz)
20
15
10
5
0
D1
RSNP
FS
Amplitude of EPSCs (Normalized)
***
**
D2
RSNP
FS
PPR
1.5
1.2
0.9
0.6
0.3
0.0

Fig 7

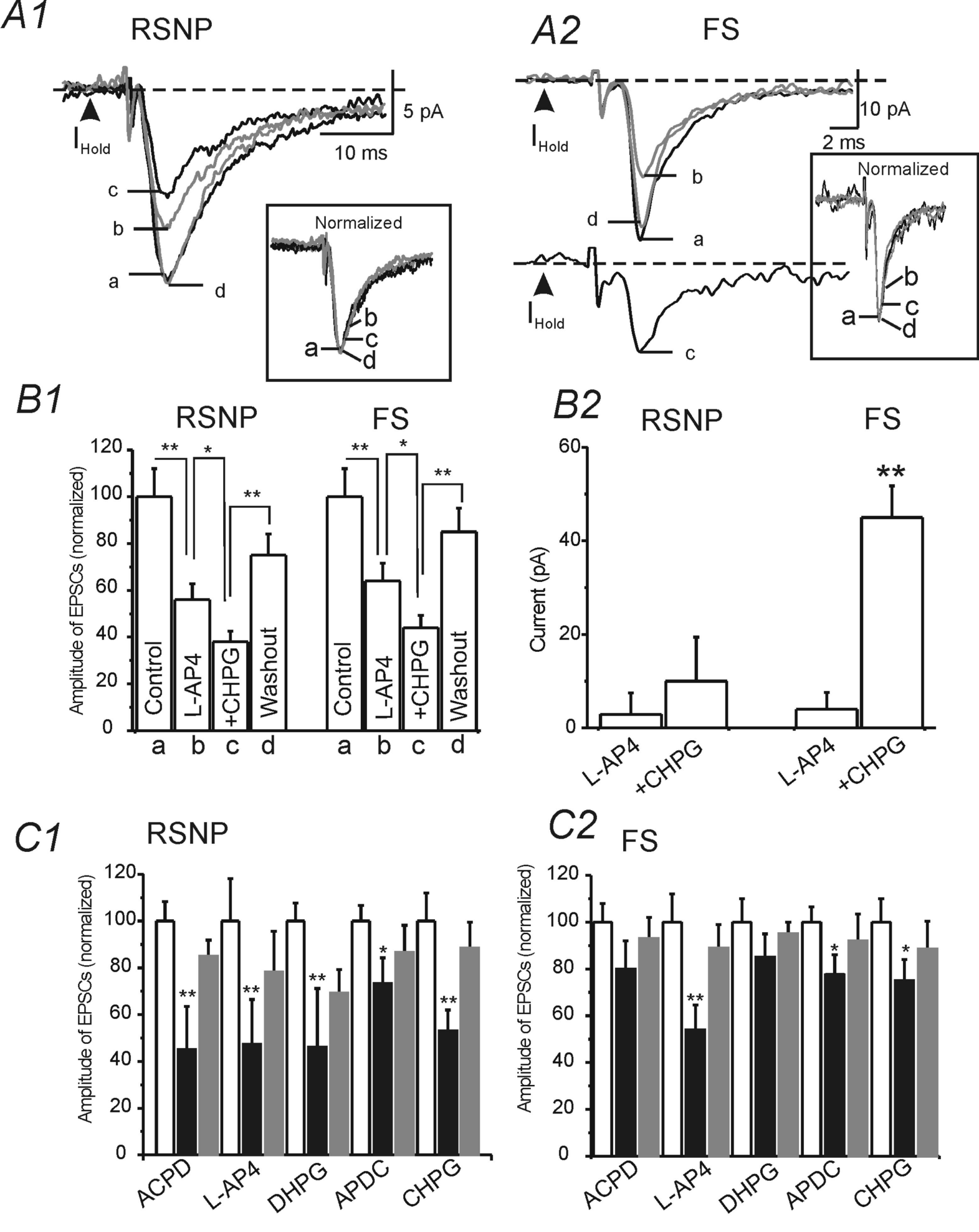
A1
RSNP
5 pA
10 ms
I Hold
c
b
a
d
Normalized
A2
FS
10 pA
2 ms
B1
RSNP
FS
Amplitude of EPSCs (normalized)
Control
L-AP4
+CHPG
Washout
B2
Current (pA)
L-AP4
+CHPG
C1
C2
ACPD
L-AP4
DHPG
APDC
CHPG

Fig 8

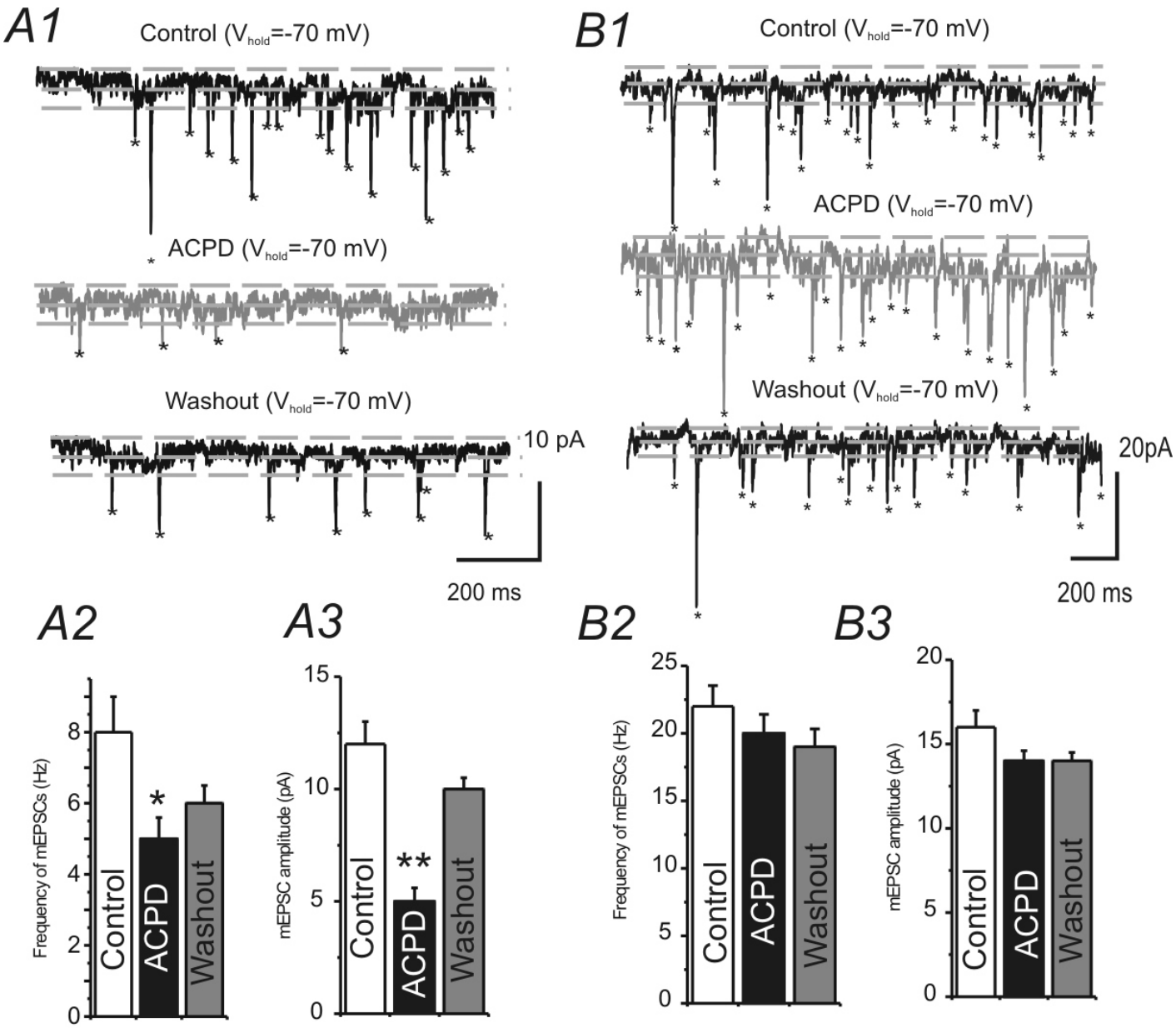

Supplemental Fig 1.

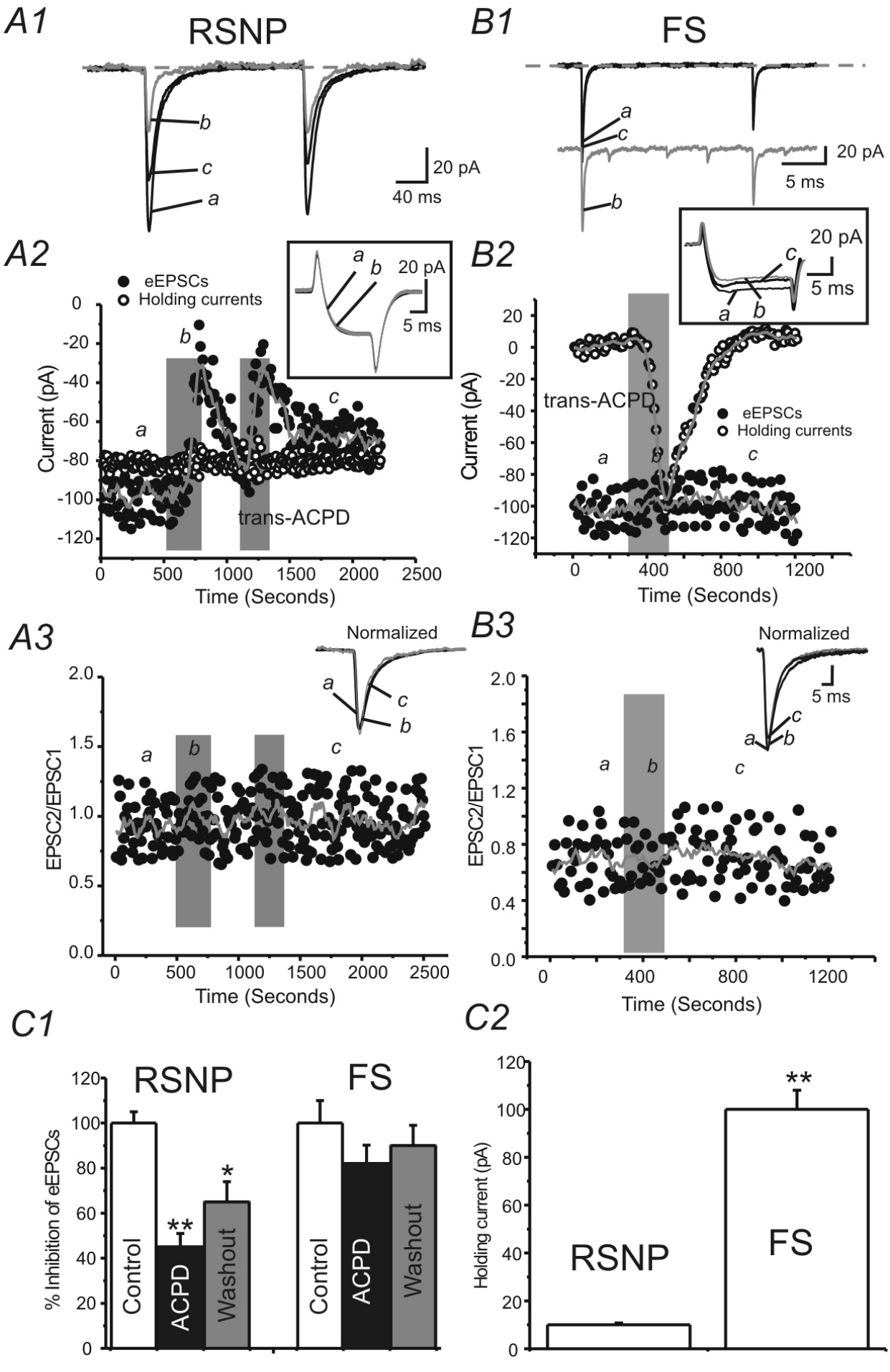

Supplemental Fig 2

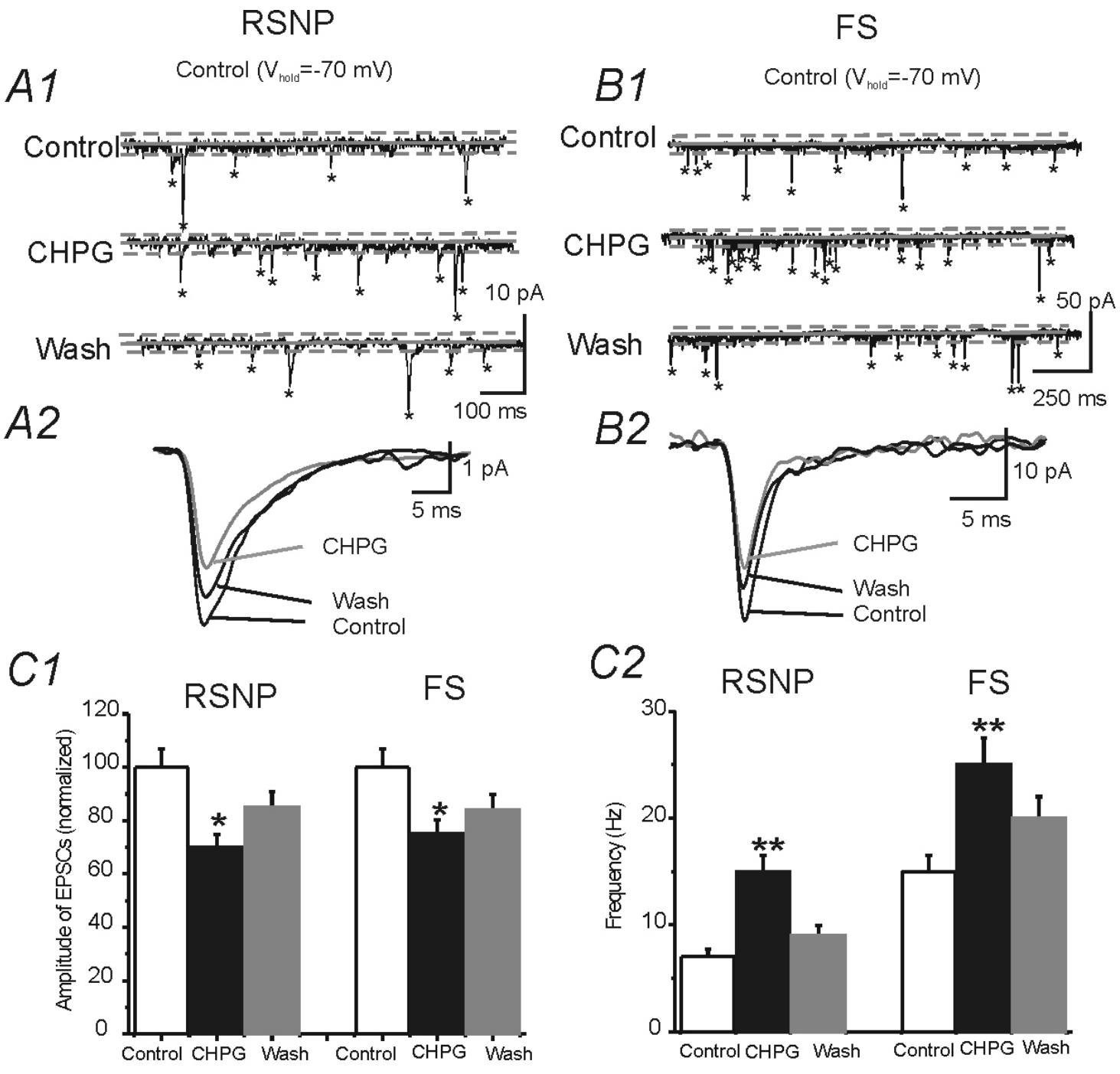

Supplemental Fig 3.